



저작자표시-비영리-변경금지 2.0 대한민국

이용자는 아래의 조건을 따르는 경우에 한하여 자유롭게

- 이 저작물을 복제, 배포, 전송, 전시, 공연 및 방송할 수 있습니다.

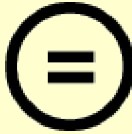
다음과 같은 조건을 따라야 합니다:



저작자표시. 귀하는 원저작자를 표시하여야 합니다.



비영리. 귀하는 이 저작물을 영리 목적으로 이용할 수 없습니다.



변경금지. 귀하는 이 저작물을 개작, 변형 또는 가공할 수 없습니다.

- 귀하는, 이 저작물의 재이용이나 배포의 경우, 이 저작물에 적용된 이용허락조건을 명확하게 나타내어야 합니다.
- 저작권자로부터 별도의 허가를 받으면 이러한 조건들은 적용되지 않습니다.

저작권법에 따른 이용자의 권리는 위의 내용에 의하여 영향을 받지 않습니다.

이것은 [이용허락규약\(Legal Code\)](#)을 이해하기 쉽게 요약한 것입니다.

[Disclaimer](#)

Thesis for the Degree of Master of Engineering

**Development of Copper-
impregnated Corncob Activated
Carbon for the Adsorption of H₂S,
NH₃ and TMA: Application to
Indoor Air Purification**

By

Tesfay Berhe Gebreegziabher

Department of Materials Science and Engineering

College of Engineering

Pukyong National University

August 2019

Development of Copper-impregnated Corncob Activated Carbon for the Adsorption of H₂S, NH₃ and TMA: Application to Indoor Air Purification

**(H₂S, NH₃ 및 TMA 흡착을 위한 옥수수 속대
활성탄 개발: 실내 공기 정화 응용에 관한
연구)**

Advisor: Prof. Ki Woo Nam

By

Tesfay Berhe Gebreegziabher

A Thesis Submitted in Partial Fulfillment of the Requirements for the
Degree of Master of Engineering

Department of Materials Science and Engineering

College of Engineering

Pukyong National University

August 2019

Development of Copper-impregnated Corncob Activated Carbon for the Adsorption of H₂S, NH₃ and TMA: Application to Indoor Air Purification

A Dissertation by

Tesfay Berhe Gebreegziabher

Approved by:

Jun Heok Lim_(Chairman)

Hee Rok Jeong_(Member)

Ki Woo Nam_(Member)

August 2019

Abstract

황화수소 (H_2S), 암모니아(NH_3) 및 트리메틸아민(TMA) 같은 휘발성 유기 화합물은 급성 및 만성적인 건강 문제, 환경 문제를 일으키는 것으로 알려져 왔다. 본 연구에서는 실내 공기에 존재하는 H_2S , NH_3 및 TMA를 흡착하기 위하여 옥수수속대로 만든 탄소를 KOH로 활성화탄을 제조하였다. 이 때 제조한 활성화탄의 흡착제거 성능을 향상시키기 위하여, 구리 금속 혼합물을 활성화탄 표면에 담지하였다. 제작된 활성화탄의 특성화는 BET, Pore volume, SEM, EDS, TGA, proximate 및 ultimate 분석을 실시하였다. 흡착 과정을 분석하기 위하여 Langmuir, Freundlich 및 Temkin의 isotherm model을 검토하였다. 본 연구의 결과는 Langmuir 모델에 의하여 가장 잘 설명되는 것으로 나타났다. Adsorption Kinetics 분석 결과는, pseudo-second order kinetic model이 NH_3 와 TMA에 대하여 가장 우수하였으며, pseudo-first order model은 H_2S 에 가장 적합한 것으로 나타났다. 옥수수속대 활성화탄에 의한 H_2S , NH_3 및 TMA의 흡착 능력은 각각 154.96 mg/g, 181.24 mg/g, 313.27 mg/g이었. 옥수수속대 활성화탄은 실내의 유독 가스를 제거할 수 있는 활성화탄이라 판단된다.

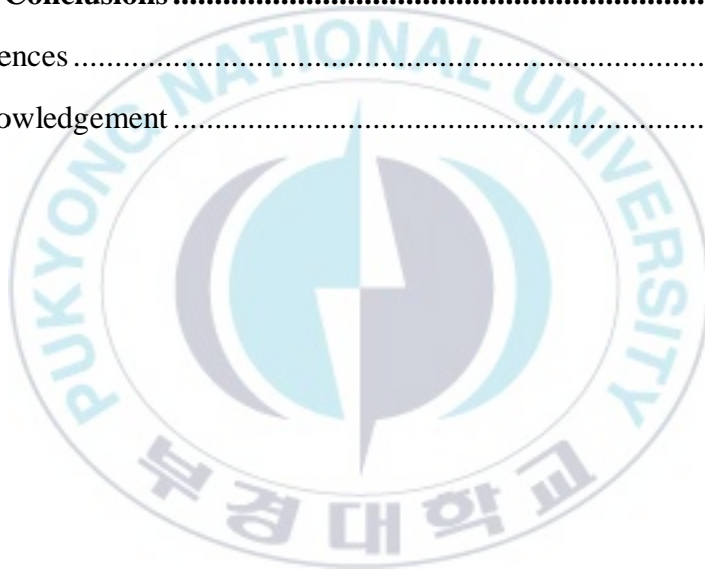
Keywords: Adsorption; Corncob activated carbon; H_2S ; Isotherm, Kinetics, NH_3 ; TMA

Contents

| | |
|--|----------|
| Abstract | i |
| List of Figures | v |
| List of Tables..... | vii |
| 1. Introduction | 1 |
| 1.1. Problem Statement | 1 |
| 1.2. Objectives | 3 |
| 2. Literature Review | 4 |
| 2.1. Health Effects of H ₂ S, NH ₃ and TMA | 4 |
| 2.1.1. Hydrogen Sulfide Health Effects | 4 |
| 2.1.2. Ammonia Health Effects | 5 |
| 2.1.2. Trimethylamine Health Effects..... | 6 |
| 2.2. Removal of Toxic Gases | 6 |
| 2.2.1. Removal of Hydrogen Sulfide | 6 |
| 2.2.2. Removal of Ammonia | 7 |
| 2.2.3. Removal of Trimethylamine..... | 8 |
| 2.3. Factors Affecting Adsorption | 8 |
| 2.3.1. Nature of the Adsorbent | 8 |
| 2.3.2. Nature of the Adsorbate | 9 |
| 2.3.3. Solution pH..... | 10 |
| 2.3.4. Temperature..... | 10 |
| 2.4. Types of Activated Carbon Preparation Methods..... | 11 |

| | | |
|-----------|--|-----------|
| 2.4.1. | Physical Activation | 11 |
| 2.4.2. | Chemical Activation | 11 |
| 2.5. | Corncob as Biomass Source of Activated Carbon | 16 |
| 3. | Experimental | 17 |
| 3.1. | Preparation of Corncob Activated Carbon | 17 |
| 3.1.1. | Carbonization Process | 17 |
| 3.1.2. | Activation Process | 18 |
| 3.2. | Characterization of Corncob Activated Carbon | 19 |
| 3.3. | Batch Adsorption Experiments | 21 |
| 3.4. | Regeneration of Spent Adsorbent | 24 |
| 4. | Results and Discussions | 25 |
| 4.1. | Characterization of the Adsorbent | 25 |
| 4.1.1. | Surface Morphology Characterization | 25 |
| 4.1.2. | Textural Characteristics | 27 |
| 4.1.3. | Proximate and Elemental Analysis | 30 |
| 4.1.4. | Thermal Characteristics | 32 |
| 4.2. | Adsorption Process | 34 |
| 4.2.1. | Effect of Initial Concentration on H ₂ S, NH ₃ and TMA Adsorption | 38 |
| 4.2.2. | Effect of Contact Time on the Adsorption Rate of H ₂ S, TMA, and NH ₃ | 39 |
| 4.3. | Equilibrium Adsorption Isotherm Linear Fitting Studies | 41 |

| | | |
|-----------|---|-----------|
| 4.3.1. | The Langmuir Adsorption Isotherm | 42 |
| 4.3.2. | The Freundlich Adsorption Isotherm Model..... | 49 |
| 4.3.3. | The Temkin Adsorption Isotherm Model..... | 50 |
| 4.4. | Adsorption Kinetics Study | 51 |
| 4.4.1. | Pseudo-first Order Kinetic Model..... | 51 |
| 4.4.2. | Pseudo-second Order Kinetics Model..... | 53 |
| 4.4.3. | Intra-particle Diffusion Model..... | 54 |
| 4.5. | Filter Regeneration Process | 57 |
| 5. | Conclusions | 60 |
| | References | 62 |
| | Acknowledgement | 74 |



List of Figures

| | |
|---|----|
| Figure 3.1. The experimental apparatus for the synthesis of corncob activated carbon..... | 18 |
| Figure 3.2. Overview of corncob activated carbon preparation process | 19 |
| Figure 3.3. Adsorption experiment (a) Preparation of activated carbon filter (b) adsorption experimental chamber | 22 |
| Figure 4.1. SEM of (a) raw corncob, (b) CAC400-800, (c) CAC400-850, (d) CAC450-800, (e) CAC450-850..... | 26 |
| Figure 4.2. (a) Nitrogen adsorption-desorption isotherms, (b) Cumulative pore volume, (c) DFT method pore size distribution for different corncob activated carbons. | 30 |
| Figure 4.3. Thermal characteristics of samples (a) Thermogravimetric analysis, (b) Differential thermal analysis, (c) Van Krevelen diagram of different corncob activated carbons[52]. | 33 |
| Figure 4.4. Adsorption performance of different corncob activated carbon filters for (a) H ₂ S, (b) NH ₃ and (c) TMA..... | 36 |
| Figure 4.5. EDX of CAC450-800 filter, (b) EDX of H ₂ S adsorbed CAC450- 800 filter, (c) EDX of NH ₃ adsorbed CAC450-800 filter and (d) EDX of TMA adsorbed CAC450-800 filter..... | 37 |

| | |
|---|----|
| Figure 4.6. (a) Effect of Adsorbate dose on the removal capacity of adsorbent, (b) Effect of contact time on the adoption performance of CAC450-800 activated carbon..... | 41 |
| Figure 4.7. Linear fitting plots of Langmuir adsorption model. (a) H ₂ S, (b) NH ₃ and (c) TMA..... | 46 |
| Figure 4.8. Linear fitting plots of Freundlich adsorption model. (a) H ₂ S, (b) NH ₃ and (c) TMA..... | 47 |
| Figure 4.9. Linear fitting plots of Temkin adsorption model. (a) H ₂ S, (b) NH ₃ and (c) TMA..... | 48 |
| Figure 4.10. Kinetics study. (a) Pseudo-first order kinetics of H ₂ S, NH ₃ and TMA, (b) Pseudo-second order kinetics of H ₂ S, NH ₃ and TMA | 54 |
| Figure 4.11. Intraparticle diffusion model for the adsorption of H ₂ S, NH ₃ and TMA..... | 56 |
| Figure 4.12. Adsorption performance of a regenerated corncob activated carbon filter..... | 59 |

List of Tables

| | |
|---|----|
| Table 4.1 Textural properties of different CACs | 29 |
| Table 4.2 Proximate and elemental analysis (* = % obtained by difference) | 32 |
| Table 4.3. Adsorption isotherm constants and determination coefficients of H ₂ S, NH ₃ and TMA | 45 |
| Table 4.4 Kinetic parameters, constants and coefficients of determination of H ₂ S, NH ₃ and TMA | 57 |



1. Introduction

1.1. Problem Statement

The duration of people's stay in indoor environments is continuously increasing. There is a growing concern about indoor air quality since the recently different researches reported that indoor levels of some pollutants are higher than the corresponding outdoors[1]. The U.S. Environmental Protection Agency (EPA) report shows that the average time US citizens spent daily in different microenvironments, is 22.3 h [2]. In Germany, the German Environmental Survey 1990/1992 (GerES II) reported that this duration was about 20.9 h [2] and Korean people spend time indoors about 16.0 to 17.8 h[2]. Hence, indoor air quality has been considered as an important factor in determining health and welfare [2]–[5]. Malodorous compounds surrounding us in daily life such as sulfur and nitrogen-containing compounds, which include hydrogen sulfide, ammonia and trimethylamine are responsible for indoor air pollution[6].

In all scenarios mentioned above, there is a significant interest and need in developing an air filtration unit that can adsorb H_2S , NH_3 and TMA effectively[7]–[11]. Numerous techniques have been applied to remove toxic compounds such as membranes[12], catalytic oxidation[13], biological method [6], scrubbing[14] and electrochemical method[15]. Among them,

adsorption is widely used because of its high removal potential, flexibility of its operation and low maintenance costs.

In the literature, several types of adsorbents have been previously investigated for H₂S, NH₃ and TMA adsorption such as petroleum coke [11], biochar[16], sludge adsorbent [17] zeolite [18], fibrous polymeric ionic liquids [19] and biomass activated carbon[20]. Among these, an activated carbon is emerging as the most effective solution due to its high surface area and low cost [10]. There are different agricultural byproduct sources of activated carbon such as corncob. The International Grains Council (IGC) report shows that the annual global corn production was up to 1.13 billion tons from 2016/2017[18] and this yields large amount of corncob waste. Majority of the corncobs are simply burnt down directly in the agricultural field or used as household fuel in the rural areas. This leads to the release of various contaminants and causes a serious environmental disaster.

Therefore, the reuse and utilization of corncobs is crucial to minimize the emission of greenhouse gases. Many studies have reported that corncobs and the carbonized products can be utilized as potential adsorbents for various pollutants. Zhu et al. [22] employed corncob-based activated carbons for the removal of toluene from waste gas. El-Sayed et al. [23] assessed the adsorption methylene blue (MB) using corncob activated carbon prepared by chemical activation with phosphoric acid.

Moreover, other researchers used corncob activated carbon for hydrogen storage[24], 2,4-dichlorophenoxyacetic acid adsorption[25], monoethylene glycol adsorption[26], removal of Cu(II) from aqueous solution[27], removal of ammonium from groundwater[7]. Nevertheless, to the best of our extensive literature survey, there were no related studies of corncob-based activated carbons as adsorbents for hydrogen sulfide gas, gaseous ammonia, and gaseous trimethylamine.

1.2. Objectives

The objective of this study is to investigate the performance of corncob-based activated carbon in the removal of H₂S, NH₃ and TMA from indoor areas. In this work, four different activated carbons were chemically synthesized from corncob with potassium hydroxide and used as adsorbents to remove hydrogen sulfide, gaseous ammonia and gaseous trimethylamine at room temperature. In order to understand the adsorption process, the equilibrium and kinetic data on batch adsorption studies were conducted by varying the adsorption conditions like contact time, initial gas concentration and application of copper catalyst. Finally, the study evaluated the feasibility of regeneration and reusability of spent adsorbents.

2. Literature Review

2.1. Health Effects of H₂S, NH₃ and TMA

2.1.1 Hydrogen Sulfide Health Effects

Hydrogen sulfide (H₂S) also known as sewer gas is an extremely flammable and toxic colorless gas known for its pungent “rotten egg” odor. Hydrogen sulfide is a byproduct of the decomposition of organic materials, such as putrescible commercial waste or sewage sludge. It also occurs naturally in sewers, septic tanks, manure pits, well water, and dry wells[5], [6].

Because it is heavier than air and can move along the ground, hydrogen sulfide tends to pool in low-lying, poorly ventilated spaces. Its presence or potential presence can make work in these spaces extremely dangerous. At very low concentrations, H₂S has the characteristic of malodorous nature. However, exposure to about 100 ppm, it may lead to loss of sense of smell and can create the false impression as if there is no hazard. Since the toxicity threshold of H₂S is around 10 ppm, exposure to concentrations around 300 ppm for 30 min is sufficient to cause unconsciousness. A single breath at a concentration of about 500 – 700 ppm can lead to an immediate death[28].

2.1.2. Ammonia Health Effects

Ammonia (NH_3) is a colorless, corrosive, alkaline gas that has a very pungent odor. It is one of the gases regarded a serious indoor pollutant. Ammonia is one of the commonly used materials that needs special concern in hazard control[29]. It is used as household cleaning product, fertilizer, and refrigerant [30]. Ammonia is also widely used in the manufacture of explosives, the textile and fiber industries, metal treatment as a corrosion inhibitor, and water and aqueous effluent treatments. Exposure to ammonia can lead to a serious health impact. The odor detection level ranges from 5 to 53 ppm[29].

The New York State Department of Health[31] states that ammonia can make immediate interaction when it contacts with available moisture in the skin, oral cavity, eyes, respiratory tract, and especially with the mucous surfaces and forms the very caustic ammonium hydroxide. Ammonium hydroxide leads to the necrosis of tissues by disrupting of cell membrane lipids (saponification), which finally causes cellular destruction. As cell proteins are denatured, water is extracted, which leads to an inflammatory response and further cell damage. Concentrations of a few hundred ppm (v/v) can irritate the eyes and mucous membranes, but exposures at a few thousands of ppm (v/v) can be lethal, due to respiratory failure[30].

2.1.3. Trimethylamine Health Effects

The trimethylamine with a chemical formula $N(CH_3)_3$ is a volatile, colorless, and flammable tertiary amine with a strong rotten-fish odor[29]. TMA is released into the ambient air from the industrial manufacturing processes, leading to the poor air quality and adverse health impacts. In addition, TMA has been reported as a carcinogenic compound[32]. Nowadays, the study on environmental friendly and sustainable technologies is a serious global concern, especially application of agricultural waste to enhance the value of the material and to reduce waste production[32].

2.2. Removal of Toxic Gases

2.2.1. Removal of Hydrogen Sulfide

Léa Sigot et al [18] studied the adsorption of hydrogen sulfide by retention on a zeolite adsorbent and it was revealed that H_2S was converted into elemental sulfur with the zeolite. This process involves H_2S adsorption at the surface of zeolite, dissociation of H_2S in water contained in the zeolite pores, then finally oxidation to give elemental sulfur. The drawback of this process was the formation of an elemental sulfur, which hinders the thermal regeneration of the spent zeolite. Guofeng Shang et al [33] determined the adsorption capacity of hydrogen sulfide on the surface of three different

biochar prepared from camphor, bamboo, and rice hull at 400 °C by oxygen-limited pyrolysis. Fen LI et al[17] also investigated the potential of sludge adsorbent for the removal of hydrogen sulfide. Other researchers used petroleum coke activated carbon[11], V-Cu-O mixed oxides bronzes[13], and bacterial deodorant [6] for the successful removal of hydrogen sulfide.

2.2.2. Removal of Ammonia

In the literature, different methodologies have been applied to remove ammonia. Ebrahim Rezaeia et al[34] evaluated the removal of gaseous ammonia using different metal oxide nano-particles particularly MgO, CuO, ZnO, and TiO₂ along with activated charcoal[10] The adsorption test was conducted in a packed column and TiO₂ has revealed the maximum adsorption potential (6.87 mgg⁻¹).

The authors also investigated the removal of gaseous ammonia using nano TiO₂-activated carbon composites. The ammonia adsorption potential of TiO₂ nano-particles in 30% TiO₂-AC composite was better than a commercial 40 nm TiO₂ nano-particles, due to the relatively smaller size of TiO₂ nano-particles mixed with AC. The addition of TiO₂ to AC modified the multilayer adsorption of NH₃ to a monolayer adsorption. Moreover, Qinan Song et al[15], Weihua Zheng et al [35], Takuya Mochizuki et al[11] studied the removal of ammonia using electrochemical method, activated carbon fiber composites, petroleum coke activated carbon respectively.

2.2.3. Removal of Trimethylamine

Phattara B. and Paitip T[32] investigated the effect of alkanes, fatty acids, and aromatic compounds in waxes during the adsorption of trimethylamine using biomaterials. Different plant leaf materials were chosen to be used as dried biomaterial adsorbents particularly for polar gaseous trimethylamine (TMA) adsorption. Biomaterial adsorbents (plant leaves) were able to completely remove gaseous TMA (100 ppm) in 24 h. *Sansevieria trifasciata* was the most efficient plant leaf material while *Pterocarpus indicus* had the least effectiveness in TMA adsorption. In addition, Takahiro H. et al[6] employed a bacterial deodorant to effectively remove TMA.

2.3. Factors Affecting Adsorption

There are several factors that affect the adsorption process. The nature of adsorbent, the nature of adsorbate, pH and temperature of the adsorption process have a critical impact on the efficiency of adsorption.

2.3.1. Nature of the Adsorbent

Since adsorption process is regarded as a surface phenomenon, the rate of adsorption greatly depends nature of the adsorbent such as the available total surface area and pore volume to the adsorption process[36][11]. In

addition, the adsorption capacity is highly influenced by the physicochemical nature of the surface of carbon. Hence, the special selection or preparation conditions of activated carbons for specific applications should be considered.

2.3.2. Nature of the Adsorbate

The inherent characteristics of the adsorbate like its rate of transport towards the adsorbent material has a strong effect on the adsorption process[36]. The molecular size of the adsorbate is also a significant factor. The rate of uptake of adsorbates from adsorption solution by porous adsorbents is related to the molecular size. Adsorbates with smaller molecular size have high rate of adsorption. In contrast to the effect of molecular size, the geometrical and structural variation of the molecules have low effect on the equilibrium conditions[36]. In addition, ionization is considered to have considerable effect on the uptake capacity especially to molecules, which are easily ionizable.

For instance, compounds like amines, fatty acids, and pesticides can be easily ionized at appropriate conditions of pH. The ionization property of many adsorbates is believed have a significant effect in the activated carbon adsorption process. This is because activated carbon mostly contains a net negative charge. Researchers observed that a polar solute have high tendency to be well adsorbed by a polar adsorbent[3].

2.3.3. Solution pH

The removal capacity of adsorbates from aqueous solution depends on the pH of the solution[37][23]. Hydrogen and hydroxide ions are strongly adsorbed by activated carbon. Hence, the adsorption of other ionic molecules is affected by the pH of the adsorption solution. The adsorption of organic adsorbates from the aqueous solution can be enhanced by decreasing the pH. As the solution pH gets low, negative charges on the surface of the activated carbon can be neutralized. Hence, more available active sites can be released of the carbon. This may vary from activated carbon to activated carbon based on the technique of activation and inherent composition of the raw materials.

2.3.4. Temperature

If adsorption process is exothermic, the adsorption performance of adsorbates from aqueous solution or gas phase tends to decrease with increasing temperature. Nevertheless, it should be noted that small temperature variations have little effect on the adsorption process. The rate of adsorbate uptake is associated to the temperature and activation energy of equilibrium capacity. The activation energy dependence of the adsorption is commonly represented as activation energy (E_a), and the dependence of equilibrium capacity on temperature is represented by enthalpy change (ΔH).

2.4. Types of Activated Carbon Preparation Methods

Basically, there are two different widely accepted processes that are used to prepare activated carbon: physical and chemical activation.

2.4.1. Physical Activation

Physical activation involves the release of a large quantity of internal carbon mass in order to obtain a well-developed carbon structure. Physical activation involves carbonization of a raw material followed by activation of the carbonized product using different activating agents mainly carbon dioxide and steam. The production of activated carbon in this route can be performed in two ways. The first method is a one-step activation, which performs the carbonization and activation processes simultaneously and the other route is a two-step activation that involves a separate carbonization and activation processes.

2.4.2. Chemical activation

Chemical activation process uses a variety of chemicals as dehydrating agents. These chemical agents can influence the thermal decomposition of the raw material and avoid the formation of tar, thus improving the yield of carbon. Chemical activation is performed by impregnating a carbonized

material with an excess amount of a given chemical activating agent. The most widely used activating agents are KOH, NaOH, H₂SO₄, ZnCl₂, and H₃PO₄[38]. However, chemicals such as potassium sulphide and ferric iron carbonates of alkali metals can also be used.

Special caution should be considered to carry out the impregnation process so that enough contact between the reagent and the precursor should be kept. Impregnation leads to the dehydration of the carbon skeleton thereby swelling of the interior parts of the botanic structure and this results in the formation of a porous structure[39]. The chemically impregnated precursor is then pyrolyzed in an inert atmosphere.

Essential Factors of Chemical Activation

During the chemical activation process, each activation factor has significant effect on adsorption behavior of activated carbons and in production outputs like yield and bulk density.

i. Chemical Impregnation Ratio

In chemical activation process, it is widely accepted that the impregnation ratio (ratio of the weights of the dry biomass precursor and the chemical activating agent) is one of the most important factors on activated carbon quality. The chemical activating agents commonly adopted are

dehydrating agents such as H_3PO_4 , KOH , H_2SO_4 , and ZnCl_2 in an inert atmosphere[40], which deeply penetrate into the precursor[41]. The reaction between the activating agent and the char leads to the removal of elements like carbon and this leads to creation of micropores[42]. This structural penetration of the precursor results in the production of significant number of tiny pores. Apart from the creation of the pores and size, it has a significant effect on the resulting surface area as smaller pores generally lead to larger surface area.

The general trend for many precursors is that concentration of activating agent and surface area have direct proportional relationship [43]. However, larger pores, which commonly have smaller surface area, are created when more acid activating agents are used. When pores achieve a particular size particularly in the range from mesopore to macropore, their contribution to the surface area significantly reduces. Therefore, the addition of excessive amount of activating agent may lead to destruction of the micropores and enlarge the volume of pores.

ii. Activation Time

Similar to the concentration of the activating agent, the duration of the activation process also has a major influence on the development porous activated carbon. The length of time must be sufficient to remove all the moisture content and majority of the volatile constituents in the activated

carbon precursor so that pores to develop. The end of volatile component evolution indicates the development of the fundamental pore structures. Hence, the length of the activation time should be set up to the optimum point. Because longer activation time leads to enlargement of pores and reduction of surface area.

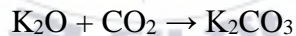
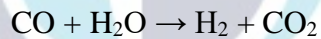
Moreover, in the economic point of view, activation time should be shorter to reduce the possible amount of energy consumption. Other duration of time dependent parameter is the yield of activated carbon. Yield of activated carbon also appeared to be significantly influenced by the duration of time during temperature treatment of the precursor[43]. The yield of the final product greatly declines after an optimum point is reached [41]. Generally, low activation time is widely accepted to achieve a higher yield due to an incomplete burn-off of the biomass sample.

iii. Activation Temperature

In the production of activated carbon, the chemical-impregnated precursor is heated at different temperatures. This application of heat to the precursor material further speeds up the thermal degradation and elimination of any volatile components. This process causes the formation of pores, which increases the surface area at the cost of the weight loss. The optimum activation temperature is selected by considering various factors such as nature of precursor and type of activating agent employed. The activation

temperature for different varieties of biomass precursors may be from 400 - 800 °C [41]. The surface area of activated carbon is greatly influenced by temperature. As activation temperature increases, reaction rate between the activating agent-KOH and carbonized materials becomes faster.

The reaction rate constant k , which is defined by the Arrhenius equation can be expressed: $k = Ae^{-E/RT}$ [7], [25], where R (8.314 J/mol K) is the ideal gas constant, A stands to the pre-exponential factor, T (K) stands temperature and E ((kJ/mol) represents the apparent activation energy of the reaction. Therefore, as the temperature increases, so does the value of k and this leads to a faster reaction rate. As a result, all kinds of pores are formed under high temperature. The following reactions commonly take place during the activation processes under high temperature.



Studies also showed that lower temperature does not favor for generation of pores because of the slow rate of reaction between the activator and

carbonized materials whereas the higher temperature probably leads to the destruction of micropores in the early stages[24], [43].

2.5. Corncob as Biomass Source of Activated Carbon

Corn is among the most widely cultivated crops in Ethiopia and all over the world. The International Grains Council (IGC) report shows that the annual global corn production was up to 1.13 billion tons from 2016/2017[44]. During the harvest of corn, large amount of corncob is produced every year. Majority of this undergoes combustion, leading to serious atmospheric pollution and resource wastes.

Cellulose, hemicellulose and a small quantity of lignin are the main chemical composition of corncob. Typically, the manufacture of high surface area activated carbon from different biomasses like corncob have attracted much attention. Corncob is an excellent renewable raw material to produce activated carbon with high surface area[45]. Different researches have used corncob activated carbon for hydrogen adsorption[24][45], monoethylene glycol adsorption[26] and dye adsorption[23] etc.

3. Experimental

3.1. Preparation of Corncob Activated Carbon

The synthesis procedure adopted in the preparation of the corncob activated carbon has two main steps, namely carbonization and activation steps. The detailed procedure of the two-step activation is described as follows based on the procedure-adopted elsewhere[5].

3.1.1. Carbonization Process

First, corncob sample obtained from local market was washed with distilled water for 30 minutes ultrasonically. The washed corncob samples were dried at 105 °C oven. Then, the dried samples were ground and sieved into powders with a typical size of approximately 700 µm. Then, the oven-dried corncobs were pyrolyzed by placing into a horizontal steel furnace (Figure 3.1) and heated to 400 and 450 °C with a ramp rate of 50 °C /min for one hour in a stream of argon gas with 2.0 L/min flow rate.

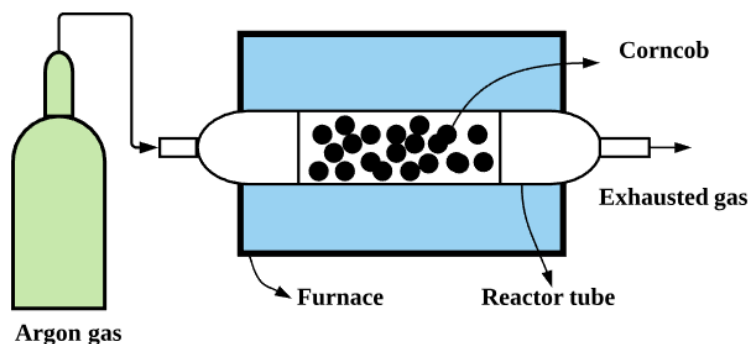


Figure 3.1. The experimental apparatus for the synthesis of corncob activated carbon

3.1.2. Activation Process

The carbonized powders were then further ground into fine powders of size less than $30\ \mu\text{m}$ with pestle and mortar grinder. To achieve the chemical alkaline activation, the carbonized corncob samples were impregnated into potassium hydroxide (KOH) in a 1:3 ratio. Then, it was continuously stirred on a hotplate in order to improve the access of the alkaline inside the pyrolyzed samples. The mixture was then dried to remove the adsorbed water at $105\ ^\circ\text{C}$ -oven.

The dried sample was transferred to a horizontal electric steel furnace and activated at a temperature of 800 and $850\ ^\circ\text{C}$ for three hours in the presence of argon gas ($2\text{L}/\text{min}$). Finally, the activated samples were repeatedly washed with deionized water to reduce the pH to about 7.0 and then oven dried at $105\ ^\circ\text{C}$ for at least $24\ \text{h}$. The as-synthesized corncob

activated carbon (CAC) samples will be hereafter represented as CAC_x-y i.e. CAC₄₀₀-800, CAC₄₀₀-850, CAC₄₅₀-800, CAC₄₅₀-850 (where x stands for carbonization temperature and y stands for activation temperature).

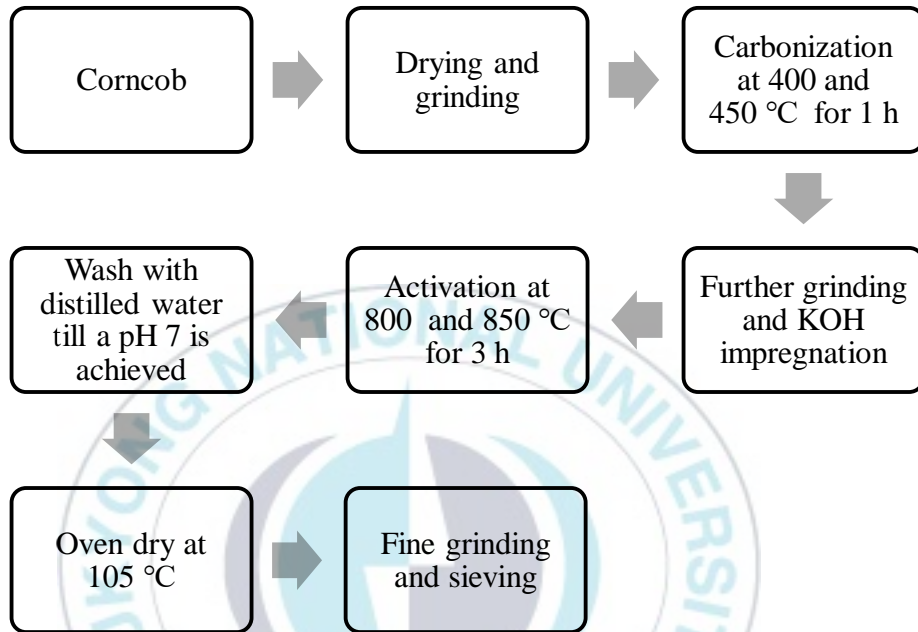


Figure 3.2. Overview of corn cob activated carbon preparation process

3.2. Characterization of Corn cob Activated Carbon

The synthesized corn cob activated carbons and raw corn cob were characterized using different characterization methods. The proximate analysis provides information regarding the moisture content and volatile contents such as lignin, cellulose, hemicellulose and other gases, which are

given off using heat treatment during carbonization[15]. In addition, the proximate analysis identifies the amount of fixed carbon and the ash content of different biomass activated carbon. On the other hand, the ultimate analysis gives information about the percent biomass composition of the sample particularly the percentage of carbon, hydrogen, nitrogen, oxygen, and sulfur[43], [46]. The elemental analysis of the activated carbon was conducted to examine the elemental composition using an Elementar Analysensysteme GmbH (vario MICRO Element Analyzer).

The surface morphology of the synthesized corncob activated carbons was examined using scanning electron microscope instrument (VEGA II, TESCAN). The textural properties of the different activated carbon samples were studied by N₂ adsorption-desorption measurements at -195.65 °C (77.35K) with automatic instrument (autosorb iQ station 1, Quantachrome Instruments) over a wide relative pressure range. The nitrogen adsorption data was used to compute the specific surface area with BET method in the relative pressure ranging from 0.02 – 0.049. The total pore volume was computed by converting quantity of N₂ adsorbed to the volume of liquid adsorbate and the micropore volume was determined using the Dubinin-Radushkevich equation.

Finally, the pore size distributions were computed using the Density Functional Theory Software according to the calculation of adsorption isotherms of different pore sizes. Energy-dispersive X-ray spectrometer

(Hitachi FE-SEM S-4800 EDX-HORIBA Emax) was used to observe the elemental composition of the filter before and after gas adsorption. This instrument particularly used to identify if the constituent elements of the adsorbate gases are available on the filter. In addition, to analyze the thermal stability of the activated carbon samples, thermogravimetric (TG) and differential thermal analysis (DTA) data were obtained using a TGA/DTA simultaneous measuring instrument (DTG-60H, Shimadzu, Japan) from the pyrolysis of corncob activated carbon samples under inert atmosphere.

3.3. Batch Adsorption Experiments

To conduct the adsorption test, an enclosed acrylic chamber (100 m³) was selected. The corncob activated carbon filter was made by mixing an organic binder, activated carbon, CuCl₂·H₂O (97.0% Cu) and deionized water in the mass ratio of 3:2:2:2 respectively. These optimum ratios were chosen after conducting several preliminary adsorption tests. To examine the role of the copper catalyst, a filter without a copper catalyst was also made by mixing activated carbon, binder and distilled water only and the sample is named as CCAC.

Then, the mixture was well stirred for about ten minutes with a hotplate stirrer so that a uniform concentration slurry is produced. Then, a polyester (PET) 7x7mm was well submerged into the slurry and a roller presser was employed to squeeze the filter to remove any extra slurry. The as-prepared

filter was placed on air to dry at ambient temperature for overnight. Before the actual adsorption test, the air-dried filter was cured at a temperature of 90 °C for about 30 min.

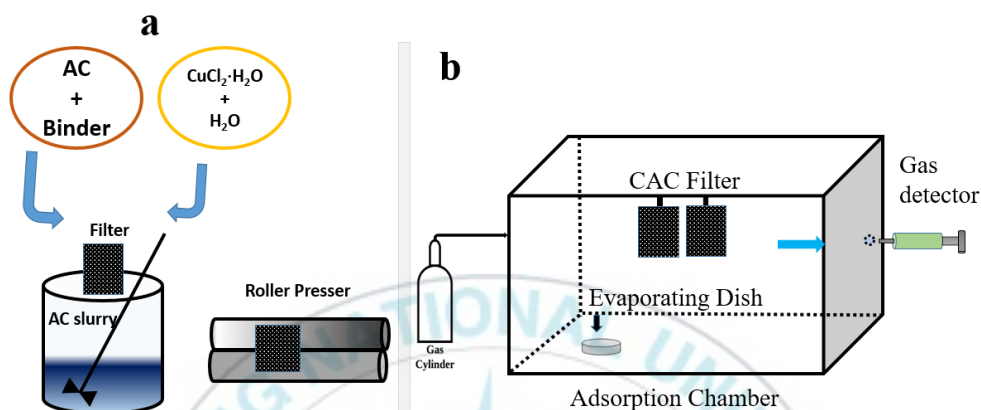


Figure 3.3. Adsorption experiment (a) Preparation of activated carbon filter (b) adsorption experimental chamber

The operating conditions of the adsorption chamber were kept at 20 °C temperature and 60% humidity based on previous study[5]. Then, the synthesized activated carbon filter was attached onto an electrically-driven fan suspended inside the adsorption chamber, which operates at 4.8 m/s velocity. The fan was installed to circulate the air inside the adsorption chamber. To undergo the adsorption experiment, one liter of H₂S gas (standard H₂S 4.02% and N₂ balance; Rigas, Korea) was injected into the

adsorption chamber and set 400 ppm initial concentration. In case of TMA, 345 μl of liquid TMA (TMA 30% mixed in water; Junsei Chemical Co., Ltd. Japan) was dropped onto a hot pad placed inside the adsorption chamber to completely evaporate and set an initial concentration of around 400 ppm.

Similarly, 0.11g of liquid NH_3 was injected onto the hot pad inside the acrylic chamber in order to set 400-ppm of NH_3 initial concentration. The electric fan (80 \times 80mm) was allowed to operate at a velocity of 4.8 m/s till the gas is completely adsorbed. The amount of H_2S , NH_3 , and TMA adsorbed inside the confined acrylic chamber was measured using colorimetric gas detection tubes (GASTEC Corporation). These tubes are very quick and accurately measure the gas concentrations. The measurement system composes a manual air-sampling pump and reactive tubes specific to the targeted gas (H_2S , NH_3 , and TMA).

The removal capacity of the synthesized activated carbon was determined by using the following mathematical expression, which relates the adsorption potential, initial adsorbate concentration and mass of adsorbent.

$$q_e = (C_i - C_f) \frac{V M_w}{m V_m} \dots \dots \dots (3.1)$$

Where, V_c (m^3), m (g), MW and V_m are the volume of adsorption chamber, mass of adsorbent, molar mass adsorbate, molar volume at 20 $^\circ\text{C}$

(24 L/mol) respectively. The adsorption efficiency of the prepared filter was evaluated using the following mathematical expression.

$$\% \text{ Adsorption} = \frac{C_i - C_e}{C_i} \times 100 \dots \dots \dots (3.2)$$

Where, C_i (ppm) and C_e (ppm) are the initial adsorbate concentration and equilibrium adsorbate concentration respectively.

3.4. Regeneration of Spent Adsorbent

In order for an adsorption technique to compete with other gas removal techniques it must be eco-friendly and economical. Thus, the recycling and reuse of adsorbent are very important issues from environment and economic point of view. To this end, this study was devoted to examine the feasibility of mild temperature regeneration of spent activated carbon using an electric furnace in the presence of an argon gas at 220 °C for 30 min[5]. The regenerated filter was used for a further toxic gas adsorption at room temperature.

4. Results and discussions

4.1. Characterization of the Adsorbent

4.1.1. Surface Morphology Characterization

To characterize the morphological surface and porosity of the prepared corncob activated carbon, scanning electron microscopy analysis (SEM) was used. The SEM analysis gives information related to the surface physical morphologies. The development of the pore system in activated carbon depends on the precursor sources and the manufacturing process. The average amount of pores greatly depends on the activation temperature and concentration of impregnation agent[47].

The scanning electron micrographs of different corncob activated carbon and the raw corncob are provided in Figure. 4.1. The SEM image of the raw corncob (Figure. 4.1a) depicts an irregular morphological surface structure with hole, which might be the space between the sample powder particles. On the contrary, the activated carbon produced at a pyrolysis temperature of 400 °C and activation temperature of 800 °C (CAC400-800) shown in Figure 4.1b developed a smooth surface accompanied with several similar size pores evenly distributed on its surface. Similarly, the activated carbons named

CAC400-850 and CAC450-800 (Figure. 4.1 c and d) show perfect porous structural development with honeycomb-like or tunnel like structures.

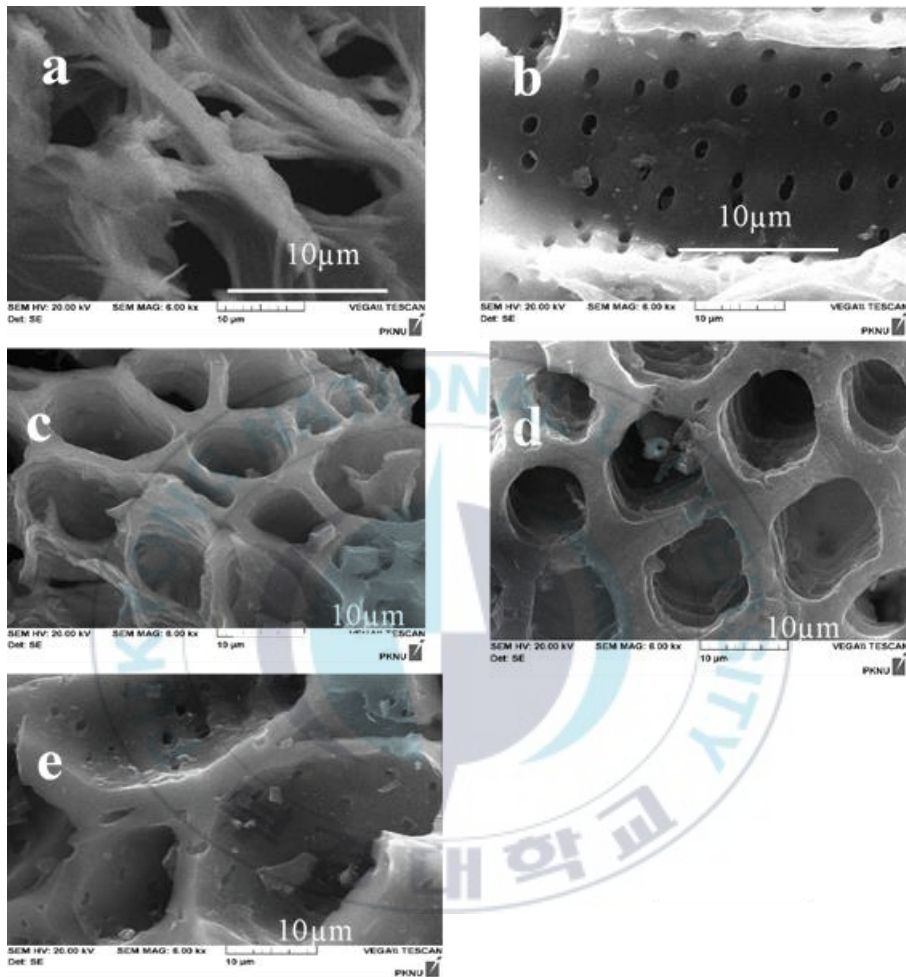


Figure 4.1. SEM of (a) raw corncob, (b) CAC400-800, (c) CAC400-850, (d) CAC450-800, (e) CAC450-850

The honeycomb shaped pores are uniformly arranged and regular and the walls of the pores are very thick with smooth and clear angle lines. The KOH impregnation caused the dehydration of the corncob skeleton and swelling of the interior structure resulting in the formation of a porous structure. The SEM micrograph of CAC450-850 (Figure.4.1e) depicts slightly bigger pores that might be due to the higher temperature. During the carbonization process majority of the volatile components of the raw corncob have been removed. This removal of the volatile components led to the development of porous structures on the surface of the activated carbon[3].

When the majority of the volatile components are emitted, a less dense morphology is developed, which is accompanied by particle size reduction. It is also obvious that the alkaline activating agent KOH significantly improved the surface morphology of activated carbon to have higher surface area, well-developed pores, and suitable porosity that enables toxic gas adsorption. These numerous pores are primarily dedicated to offer a lot of space for adsorption sites of the different gaseous molecules and for copper impregnation.

4.1.2. Textural Characteristics

The textural properties were examined using Autosorb iQ Station 1 (Quantachrome, USA) pore size and surface area analyzer. The nitrogen adsorption-desorption isotherms were obtained by degassing all the samples

at -196 °C and a partial pressure range of (6.7×10^{-6} – 0.94). The adsorption-desorption isotherms were further used for the estimation of pore size distribution, pore volume and BET surface area. Figure 4.2 depicts the nitrogen adsorption-desorption isotherms of the four corncob activated carbons. Table 4.1 reveals the different textural properties like BET specific surface area (m^2/g), average pore radius (nm), and total pore volume (cm^3/g). The nitrogen, which is adsorbed by the prepared activated carbons, mainly at low relative pressures is a typical of microporous solids[46]. The isotherms also show a hysteresis loop (Figure. 4.2a), which is attributed to the capillary condensation inside the mesopores. Hence, the isotherms reveal a type I-IV hybrid shape based on the BDDT classification; a wide knee and continued adsorption at higher relative pressures, indicates the presence of mesoporosity[48]. The shape of the graph obtained in the nitrogen isotherms of the four activated carbons is type H4, according to the IUPAC nomenclature[49], [50], which is mostly attributed to narrow slit-like pores[48].

At the relative pressure of around 0.9, the curve indicated a slight upward trend, which is an indicator of the amount of the increase of N_2 gas adsorption with increase of pressure. BET surface area was computed using a multi-point test in the partial pressure range of (0.01 – 0.072). Specific surface area is among the most important characteristics of activated carbon that has a critical effect on the adsorption capacity. The BET surface areas of CAC400-

800, CAC400-850, CAC450-800, and CAC450-850 were 1400.431 m²/g, 1532.084 m²/g, 1618.703 m²/g and 1441.431 m²/g respectively. This result indicates that the activated carbon produced at carbonization of 450 °C and activation of 800 °C provided the highest surface area.

Table 4.1 Textural properties of different CACs

| Sample Name | S _{BET} (m ² /g) | Average pore radius (nm) | Total pore volume (cm ³ /g) |
|-------------|--------------------------------------|--------------------------|--|
| CAC400-800 | 1400.431 | 0.9361 | 0.6221 |
| CAC400-850 | 1532.084 | 0.8785 | 0.6451 |
| CAC450-800 | 1618.703 | 0.9404 | 0.8117 |
| CAC450-850 | 1441.431 | 0.1003 | 0.6331 |
| CCAC[25] | 1273.910 | - | - |
| M-CCAC[7] | 1097.000 | - | - |

Micropore volume was estimated using None Linear Density Functional Theory (NLDFT) method. Total pore volume was calculated at a partial pressure of 0.99. The pore size distribution was taken from the nitrogen adsorption isotherm using NLDFT assuming slit pores. Figure. 4.2c shows the pore size distribution of the different corncob activated carbon materials. The pore size distribution followed similar pattern for all samples. A small portion of the pores has a size of around above 2 nm with a peak up to 0.04 while the remaining pore sizes were less than 2.0 nm indicating the microporous nature of activated carbon materials.

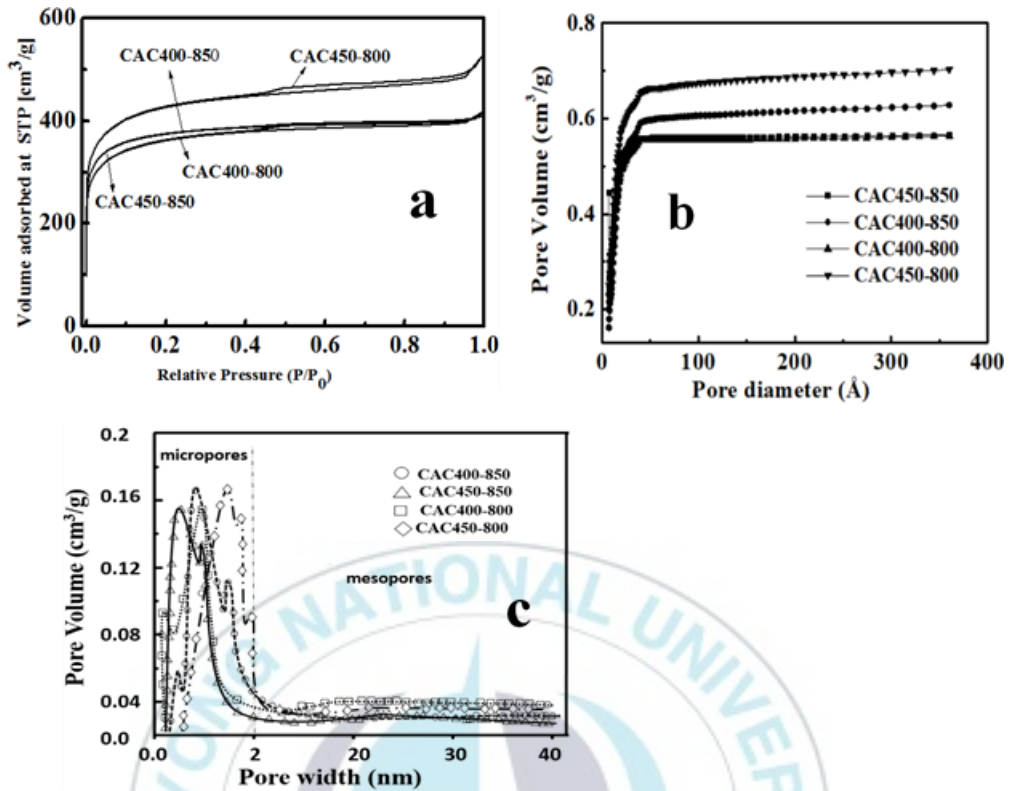


Figure 4.2. (a) Nitrogen adsorption-desorption isotherms, (b) Cumulative pore volume, (c) DFT method pore size distribution for different corncob activated carbons.

4.1.3. Proximate and Elemental Analysis

The proximate analysis and elemental composition of raw corncob and the different corncob activated carbon samples are presented in Table 4.2. The proximate analysis result shows that the raw corncob contains high

volatile combustible matter (VCM) up to 76.6 wt %. Nevertheless, after treating the corncob with potassium hydroxide and subsequent activation, the activated carbons CAC400-800, CAC400-850, CAC450-800 and CAC450-850 showed a drastic decrease to 6.7, 12.9, 11.3, 10.7 wt% respectively. On the other hand, according to the proximate analysis result provided in Table 4.2, the corncob is characterized by its rich carbon content (20.6%), which makes it desirable biomass as good precursor for activated carbon production. The fixed carbon has dramatically increased from 20.6 ± 0.8 (raw corncob) to 84.2 ± 0.5 (CAC400-800). This is mainly attributed the fact that the majority of the volatile combustible materials are given off at high temperature during pyrolysis. This result is slightly higher than the previous findings reported by Aworn et al[26] (FC =18.9%), Yaumi et al [38] (Rice husk, FC = 14.39%) and Altintig et al [51] (FC = 12.39%).

A similar trend was observed in the elemental analysis in which the carbon content increased from 40.3 (raw corncob) to 61.2% (CAC400-800). The elemental composition variation in terms of H/C and O/C ratios for raw corncob and the activated carbon products were studied with a Van Krevelen plot, as shown in Figure. 4.3. Compared to the raw corncob feedstock, the activated carbons had lower H/C and O/C ratios, which is associated with a significant structural change the raw material and the dehydration reactions taken place during the high temperature treatment[52]. In particular, the decrease in H/C and O/C ratio was more noticeable; suggesting that in the

presence of KOH dehydrogenation reactions progressed at high temperature. Furthermore, the decrease in these atomic ratios is an indication of the growth of aromatic structures in the activated carbon material. Thus, aromaticity of the product progressively increased with KOH activation[52].

Table 4.2 Proximate and elemental analysis (* = % obtained by difference)

| Sample | Proximate Analysis (wt %) | | | Elemental Analysis (wt. %) | | | | |
|-------------|---------------------------|---------|----------|----------------------------|-------|------|------|-------|
| | VCM | Ash | FC | C | S | H | N | O* |
| Raw corncob | 76.6±0.8 | 2.8±0.5 | 20.6±0.8 | 40.3 | 0.113 | 5.6 | 0.8 | 53.18 |
| CAC400-800 | 6.7±0.3 | 9.1±0.2 | 84.2±0.5 | 61.2 | 0.16 | 2.3 | 1.0 | 35.34 |
| CAC400-850 | 12.9±1.2 | 7.6±1.0 | 79.5±0.4 | 59.4 | 0.113 | 2.5 | 1.3 | 36.68 |
| CAC450-800 | 11.3±0.1 | 6.7±0.2 | 82.0±0.3 | 59.5 | 0.00 | 2.0 | 1.3 | 37.2 |
| CAC450-850 | 10.7±1.2 | 9.4±1.2 | 79.9±0.1 | 60 | 0.02 | 2.3 | 1.0 | 36.68 |
| Corncob[51] | 62.47 | 18.13 | 12.95 | 36.76 | - | 4.85 | <1 | 57.78 |
| Raw RH[38] | 66.71 | 10.13 | 14.39 | 24.77 | - | - | 1.42 | 60.5 |
| Corncob[26] | 80.2 | 0.9 | 18.9 | 48.89 | 0.00 | 6.38 | 0.18 | 44.55 |

4.1.4. Thermal Characteristics

Thermal degradation products of biomass includes volatiles, moisture, char and ash. Volatiles can also be further subdivided into gases such as light carbon monoxide, carbon dioxide, hydrogen, hydrocarbons, moisture and

tars[26]. The pyrolysis characteristics of the four different corncob activated carbons were determined using TGA/DTA simultaneous measuring instrument (DTG-60H, Shimadzu, Japan). Figure. 4.3 (a) and (b) show the thermogravimetric (TG) and Differential thermal analysis (DTA) curves obtained from pyrolysis of corncob activated carbons under inert conditions.

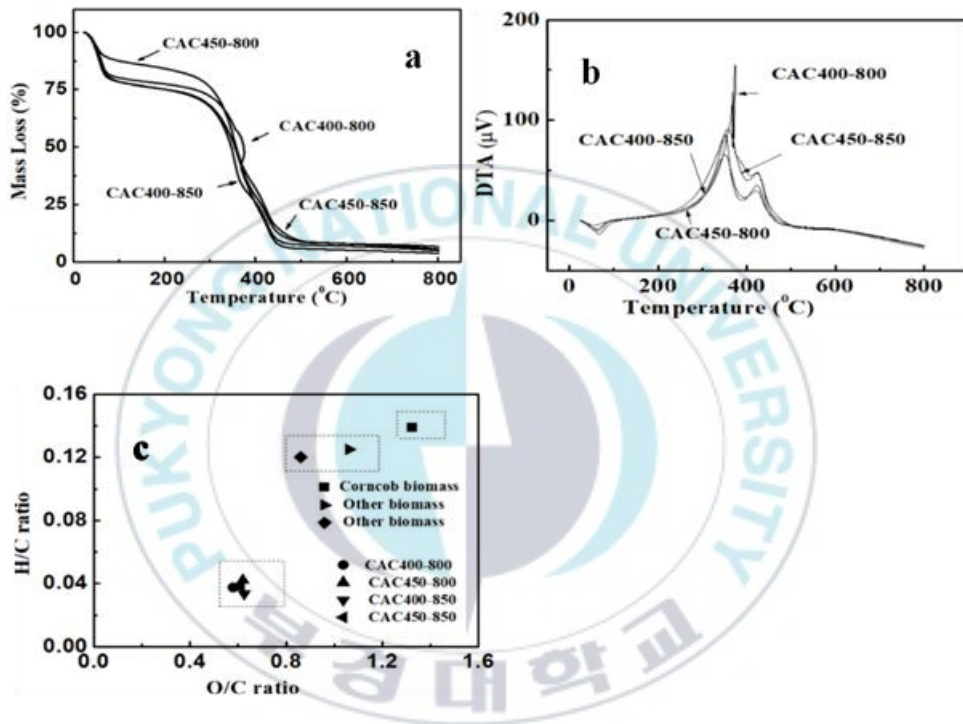


Figure 4.3. Thermal characteristics of samples (a) Thermogravimetric analysis, (b) Differential thermal analysis, (c) Van Krevelen diagram of different corncob activated carbons[52].

The thermogravimetric analysis result reveals that all the corncob activated carbon samples have similar degradation patterns. The first mass degradation step at approximately 70 to 120 °C corresponds to the evaporation of adsorbed water. The next degradation step for the activated carbons continues from 200 to 300 °C for hemicellulose then from 300 to 450 °C for cellulose degradation. Majority of the weight loss was observed at temperature between 250 and 450 °C, which might correspond to the decomposition of volatiles from the sample.

The weight of the residue remains almost constant from approximately 500 °C to 800 °C, which confirms that the corncob activated carbon samples require a minimum temperature of 440 °C to undergo a complete carbonization[26]. As illustrated by Figure. 4.3b, the maximum differential thermal loss of CAC400-800, CAC450-800, CAC400-850 and CAC450-850 were at 375 °C, 350 °C, 350 °C and 360 °C respectively.

4.2. Adsorption Process

The adsorption of H₂S, NH₃ and TMA was conducted using the metal-impregnated corncob activated carbon in a closed acrylic plastic chamber at a temperature of 20 °C and 60% humidity. To analyze the effect of the impregnated metal on the adsorption of the three gases, a filter prepared without a metal catalyst (CCAC) was employed. To this end, removal efficiency of the three gases was not satisfactory as shown in Figure. 4.4 a-c.

However, a significant toxic gas removal efficiency has been recorded using the copper impregnated corncob activated carbon. A 400-ppm initial concentration of H₂S was able to sharply drop to around 150 ppm in less than 10 min, which is more than 60% removal efficiency. After 30 min, the remaining hydrogen sulfide concentration was completely removed as provided in Figure. 4.4a. In case of the NH₃ adsorption result, a 400-ppm of NH₃ was able to decrease to around 110 ppm in 10 min. Finally, the remaining 110-ppm concentration was completely removed in 30 min as depicted in (Figure. 4.4b).

By the same token, after the adsorption of TMA with the CAC450-800, a 400-ppm concentration was drastically reduced to approximately 40 ppm in 10 min and zero ppm in 30 min (Figure. 4.4c). This rapid adsorption of the pollutant gases might be due to the combined effect of the porous activated carbon and the impregnated copper metal. The excellent porosity of the activated carbon and the catalytic effect of the copper metal played an important role during the adsorption of gases[25]. The results of the EDX analysis conducted before and after the adsorption experiment support these findings.

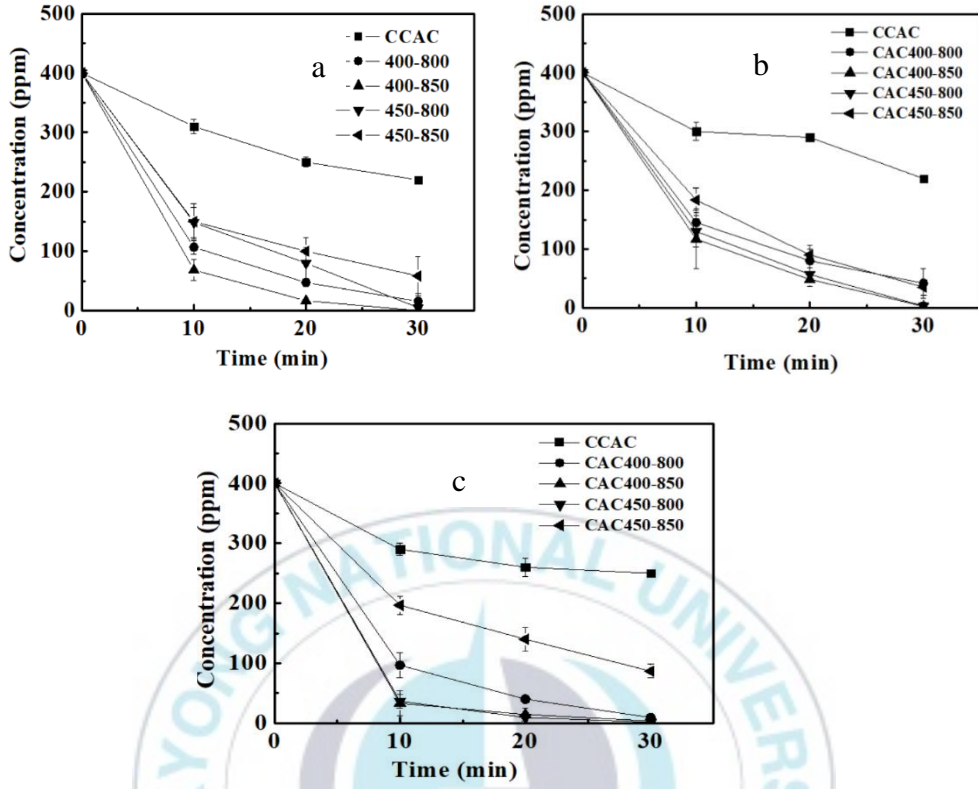


Figure 4.4. Adsorption performance of different corn cob activated carbon filters for (a) H₂S, (b) NH₃ and (c) TMA

According to the EDX analysis result obtained before gas adsorption (Figure. 4.5a), no constituent element of the H₂S, NH₃ and TMA was observed except the elemental copper, which was loaded on the activated carbon. However, the EDX spectra obtained after gas adsorption (Figure. 4.5b-d) showed the presence of “S”, which confirms the adsorption of H₂S.

Similarly, the presence of “N” confirms the adsorption of NH₃ and TMA (N(CH₃)₃) into the CAC filter. Moreover, the EDX peaks of sulfur and nitrogen were taller than other constituent elements of the activated carbon, which affirms that significant amount of H₂S, NH₃ and TMA was adsorbed onto the activated carbon. This result is in good agreement with the adsorption kinetics result provided in Figure. 4.10 below.

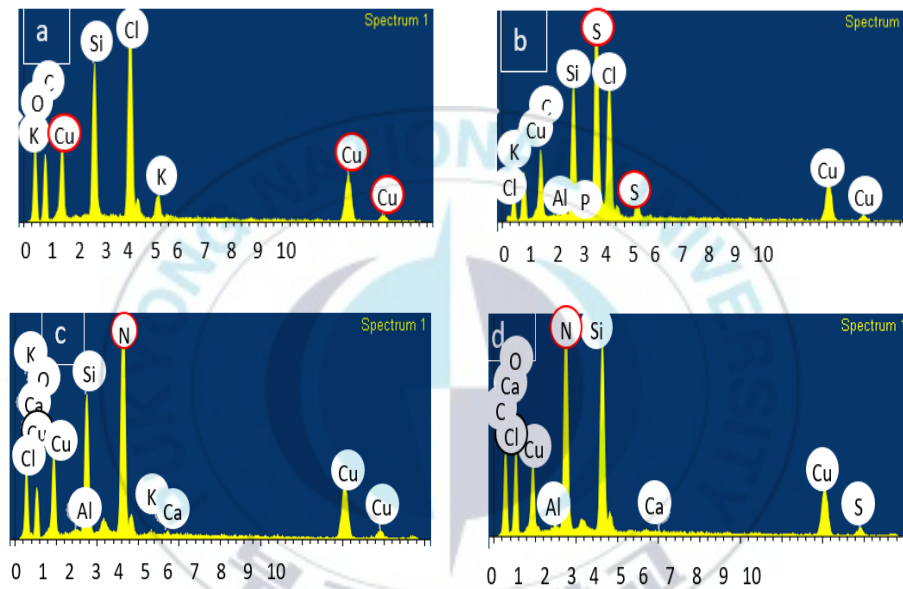


Figure 4.5. EDX of CAC450-800 filter, (b) EDX of H₂S adsorbed CAC450-800 filter, (c) EDX of NH₃ adsorbed CAC450-800 filter and (d) EDX of TMA adsorbed CAC450-800 filter

4.2.1. Effect of Initial Concentration on H₂S, NH₃ and TMA Adsorption

We studied the effect of the initial gas concentration on the adsorption removal rate by using a fixed mass of activated carbon (0.9 g) and different initial concentration of gases. The effect of initial concentration of H₂S, NH₃ and TMA on the adsorption potential of CAC450-800 was studied in wider concentration range of 400 – 2400 ppm.

The wide range of initial concentration of the three adsorbates was used to observe the adsorption performance of CAC450-800 for H₂S, NH₃ and TMA at both low and high concentrations of H₂S, NH₃ and TMA. The results showed that equilibrium adsorption capacity increased with increase in initial concentration of H₂S, NH₃ and TMA. For an increase of initial concentration of gases, a corresponding increase in equilibrium adsorption capacity observed for H₂S, NH₃ and TMA.

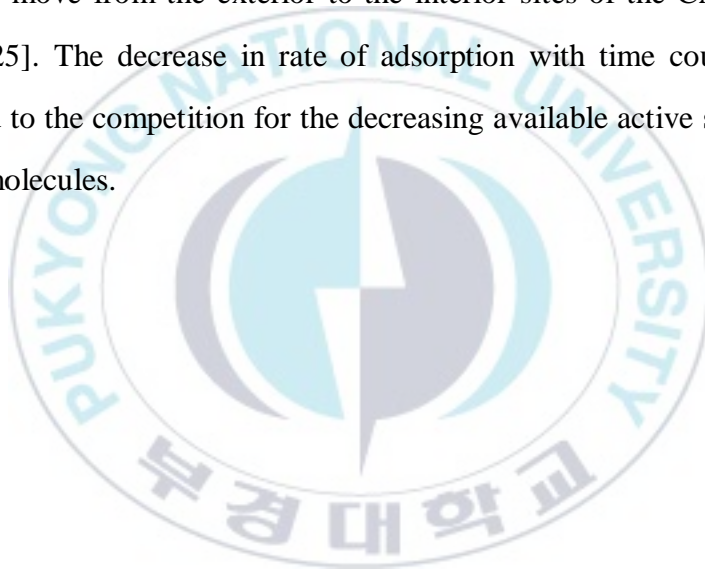
The utilization of all available active sites of the adsorbent for adsorption at higher adsorbate concentration, a large mass transfer driving force and high rate of collision among adsorbate molecules led to the increase in equilibrium adsorption capacity[25]. However, it was observed that an increase in H₂S, NH₃ and TMA initial concentration resulted to decrease in percent removal as shown in Figure. 4.6a. It can also be referred to Figure 4.6a that at extremely higher initial concentration of the H₂S and TMA, removal efficiency of the corncob activated carbon greatly decreased while still 70% removal of NH₃ was maintained at 2400-ppm initial concentration.

The decrease in removal percentage could be due to the saturation of all available active sites on the activated carbon with the increase the adsorbate concentration. On the contrary, it is worth noting that even though the percent adsorption declines with the increase of adsorbate gas concentration, the actual amount of H₂S, NH₃ and TMA adsorbed per unit mass of activated carbon increased with the increases of gas concentration.

4.2.2. Effect of Contact Time on the Adsorption Rate of H₂S, TMA, and NH₃

Contact time is one of the most important parameters that affect the adsorption potential of activated carbon. The effect of contact time on the removal of the three adsorbates using the metal impregnated corncob activated carbon is illustrated in Figure 4.6b. Longer contact time favors the adsorption efficiency until equilibrium is achieved. The experiments on the effect of contact time on the adsorption rate of H₂S, NH₃ and TMA by CAC450-800 were carried out by measuring the residual gas concentration at predetermined time intervals. Figure. 4.6b indicates the effect of contact time on the uptake efficiency of H₂S, NH₃ and TMA by CAC450-800 for the initial concentrations of 1000 ppm with CAC450-800 at 20 °C . The adsorption of H₂S, NH₃ and TMA increased with contact time and was fast during the initial stages then slowed down until equilibrium stage from 150 min, 90 min, and 180 min respectively.

After this, further increase in contact time had very little effect on the percent removal of the three gaseous adsorbates. The amount of gases adsorbed at equilibrium reflect the maximum adsorption capacity of CAC450-800 under the operating conditions. The rapid rate of adsorption observed at the beginning might be due to abundant number of vacant spaces and larger surface area of the activated carbon[46][37]. But, when equilibrium is attained, the capacity of CAC450-800 gets drained. The removal rate is then mainly controlled by the rate at which the adsorbate molecules move from the exterior to the interior sites of the CAC450-800 particles[25]. The decrease in rate of adsorption with time could also be associated to the competition for the decreasing available active sites by the gaseous molecules.



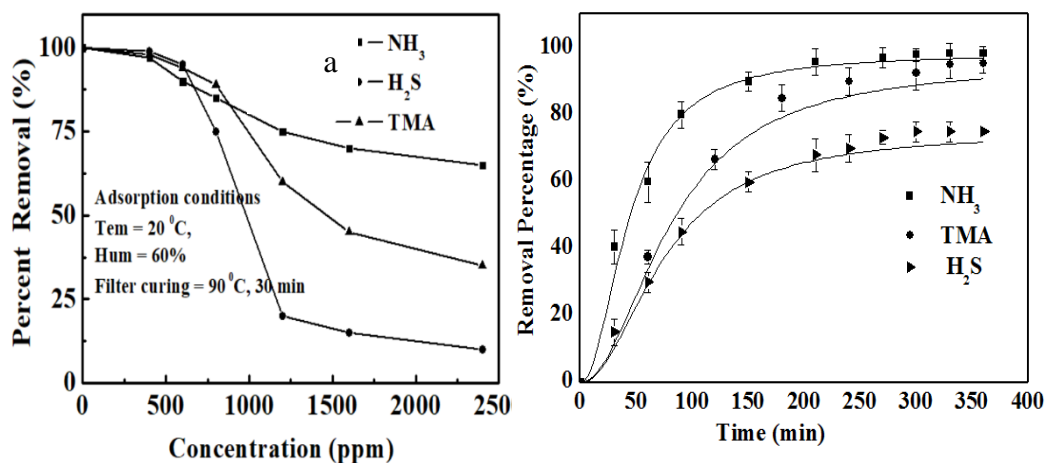


Figure 4.6. (a) Effect of Adsorbate dose on the removal capacity of adsorbent, (b) Effect of contact time on the adoption performance of CAC450-800 activated carbon

4.3. Equilibrium Adsorption Isotherm Linear Fitting studies

Adsorption occurs when an adsorbent comes in contact with adsorbate. After adsorption starts, adsorbent and adsorbate reach at equilibrium, which is called adsorption equilibrium. Adsorption equilibrium data is represented by isotherm, isobar and isostere. Adsorption isotherm is crucial in describing the interaction of adsorbate and adsorbent and helps to optimize the use of the different adsorbents. Langmuir, Freundlich and Tempkin isotherm

models were examined and their corresponding parameters are presented in Table 4.3.

4.3.1. The Langmuir Adsorption Isotherm

The Langmuir adsorption isotherm quantitatively describes the development of a monolayer adsorbate on the external surface of the adsorbent and then no further adsorption takes place after that[53]. The Langmuir isotherm is applied for monolayer adsorption model onto an adsorption surface with a fixed number of identical sites[53]–[55]. The Langmuir model commonly assumes that uniform adsorption energies onto the adsorption surface and no transmigration of adsorbate. Based upon these assumptions, Langmuir model is represented by the following mathematical expression.

$$q_e = \frac{q_m K_L C_e}{1 + K_L C_e} \dots\dots\dots(4.1)$$

Where,

C_e (mg/L) = equilibrium concentration adsorbate

q_e (mg/g) = adsorbate concentration at equilibrium

K_L (L/mg) = Langmuir isotherm constant associated with free energy of adsorption

q_m (mg/g) = the maximum adsorption capacity at monolayer coverage

However, since the linear mathematical form is widely used this expression can be converted to a linear mathematical form as:

$$\frac{1}{q_e} = \frac{1}{q_m K_L C_e} + \frac{1}{q_m} \dots\dots\dots(4.2)$$

A plot of q_e against C_e gave curves (Figure. 4.7 a-c) with high coefficient of determination (R^2) values for H_2S ($R^2 = 0.9991$), NH_3 ($R^2 = 0.9977$) and TMA ($R^2 = 0.9987$), which shows that the experimental data is well described with the Langmuir adsorption model. In addition, this model showed lower values of the residual sum of square (RSS). The essential behavior of the Langmuir isotherm can also be described using the dimensionless separation factor (R_L), which is mathematically expressed as:

$$R_L = \frac{1}{1 + K_L C_0} \dots\dots\dots(4.3)$$

Where

K_L is the Langmuir adsorption constant

C_0 is the initial concentration of adsorbate.

Here, K_L is the Langmuir constant associated to the enthalpy of adsorption via the Van'tHoff equation, and C_0 the initial concentration of

adsorbate. R_L indicates the type of isotherm: linear ($R_L = 1$), favorable ($0 < R_L < 1$), unfavorable ($R_L > 1$), or irreversible ($R_L = 0$)[53]. The evaluation of favorable adsorption condition has important contribution in optimizing an adsorbent and designing an efficient adsorption process. The value of the R_L is a criterion of favorability of adsorption when $0 < R_L < 1$, which has been extensively used for many adsorption processes[54], [56], [57][58]. The R_L values calculated in this study were found to be 0.017, 0.3284, and 0.07 for adsorption of H_2S , NH_3 and TMA respectively on CAC450-800. This indicates that Langmuir isotherm model was favorable.

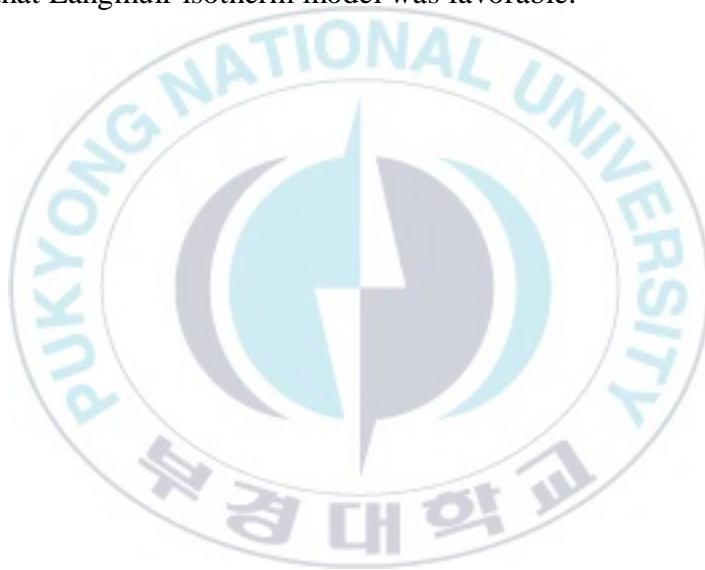


Table 4.3. Adsorption isotherm constants and determination coefficients of H₂S, NH₃ and TMA

| Model | Parameter | H ₂ S | NH ₃ | TMA |
|------------|----------------|----------------------|----------------------|----------------------|
| Langmuir | q _m | 170.5 | 4545.45 | 927.64 |
| | K _L | 39.8 | 1.20 | 4.47 |
| | R _L | 0.017 | 0.3284 | 0.07 |
| | RSS | 4.61E ⁻⁰⁸ | 9.92E ⁻⁰⁷ | 3.22E ⁻⁰⁷ |
| | R ² | 0.9991 | 0.9977 | 0.9987 |
| Freundlich | K _f | 308.07 | 4237.72 | 1404.43 |
| | n | 2.78 | 1.124 | 1.4 |
| | RSS | 0.0239 | 0.0052 | 0.0105 |
| | R ² | 0.9399 | 0.9972 | 0.9583 |
| Temkin | A _T | 7.24 | 255.35 | 75.32 |
| | b | 70.5 | 29.67 | 18.016 |
| | R ² | 0.9808 | 0.9667 | 0.9965 |
| | RSS | 70.15 | 466.90 | 74.5 |

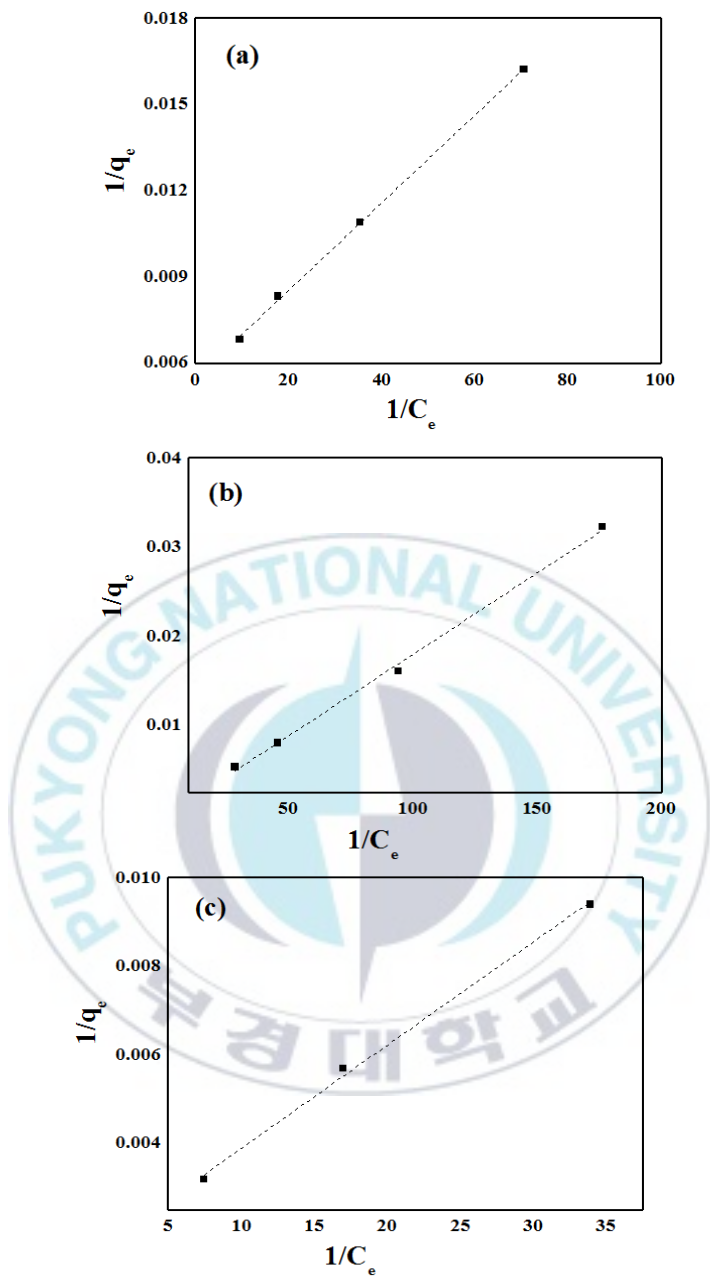


Figure 4.7. Linear fitting plots of Langmuir adsorption model. (a) H_2S , (b) NH_3 and (c) TMA

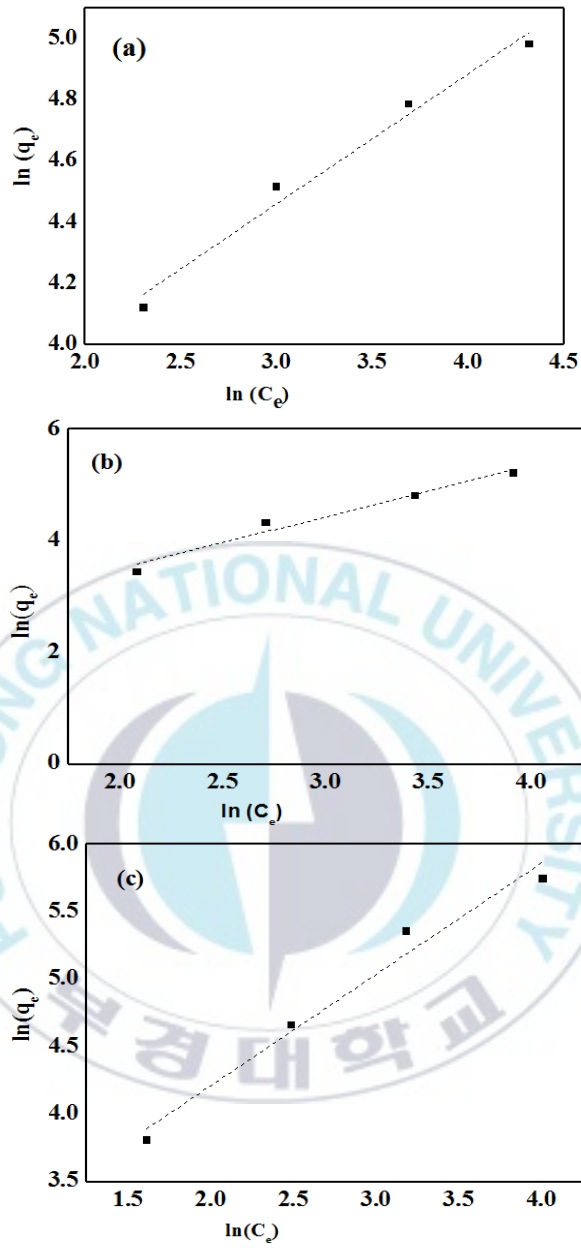


Figure 4.8. Linear fitting plots of Freundlich adsorption model. (a) H₂S, (b) NH₃ and (c) TMA

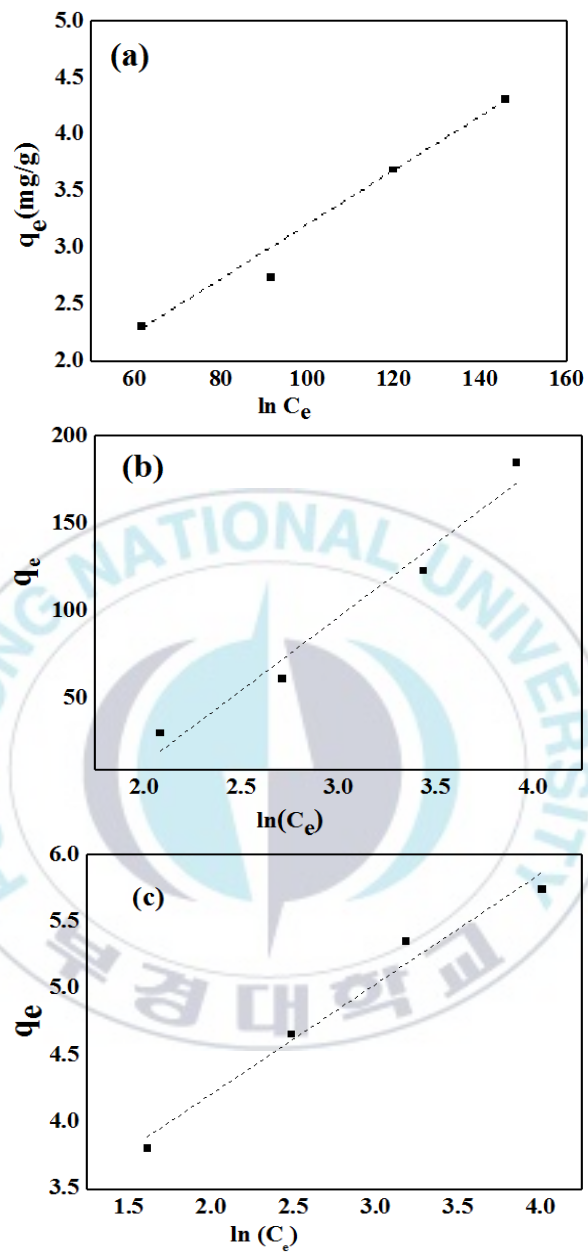


Figure 4.9. Linear fitting plots of Temkin adsorption model. (a) H_2S , (b) NH_3 and (c) TMA

4.3.2. The Freundlich Adsorption Isotherm Model

The Freundlich isotherm model uses an empirical equation to express heterogeneous systems[23], [46], [53]; it is generally characterized by the heterogeneity factor $1/n$. Therefore, the nonlinear and linear empirical equations are provided in equation 4.4 and 4.5 respectively.

$$q_e = K_f C_e^{\frac{1}{n}} \dots \dots \dots (4.4)$$

$$\ln q_e = \ln K_f + \frac{1}{n} \ln C_e \dots \dots \dots (4.5)$$

The favorability of an adsorption is also evaluated with the Freundlich's intensity factor n in the Freundlich isotherm. The adsorption is commonly classified with the values of n : good (2 - 10), moderately difficult (1 - 2), and poor (< 1)[58]. The value of the coefficient of determination (R^2) was relatively lower with a less fitted curve compared to that of Langmuir model for H_2S ($R^2 = 0.9399$), NH_3 ($R^2 = 0.9972$) and TMA ($R^2 = 0.9583$). The following mathematical equation was used to evaluate the experimental data and determine the best-fitting adsorption isotherm.

$$R^2 = \frac{\sum(q_m - \bar{q}_e)^2}{\sum(q_m - \bar{q}_e)^2 + \sum(q_m - q_e)^2} \dots \dots \dots (4.6)$$

4.3.3. The Temkin Adsorption Isotherm Model

The Temkin isotherm is commonly employed for a heterogeneous surface energy systems with non-uniform distribution of adsorption of heat[53], [59].

$$q_e = \frac{RT}{b} \ln(A_T C_e) \dots\dots\dots(4.7)$$

This equation may also be linearized and rewritten as follows:

$$q_e = \frac{RT}{b} \ln A_T + \frac{RT}{b} \ln C_e \dots\dots\dots(4.8)$$

Where,

b = Temkin isotherm constant

A_T = Temkin isotherm equilibrium binding constant (L/g)

T = Temperature at 298K

R = universal gas constant (8.314J/mol/K).

The plot of q_e versus $\ln C_e$ gave good fitting curves for three of the adsorbate. Nevertheless, Langmuir isotherm model best fitted with highest adsorption capacity for H₂S, NH₃ and TMA.

4.4. Adsorption Kinetics Study

A kinetic study was carried out for the prediction of adsorption rate constants, equilibrium adsorption capacity and adsorption mechanism. The variation in adsorption potential with contact time was analyzed to characterize the adsorption kinetics. The experimental results were studied using kinetic models like, the pseudo-first order, pseudo-second order, and the intraparticle diffusion model. These models were used to describe H₂S, NH₃ and TMA adsorption as well as predict the adsorption mechanisms participated in the removal of these gaseous adsorbates from indoor air. Table 4.4 shows the kinetics models parameters of the three models.

4.4.1. Pseudo-first Order Kinetic Model

The pseudo-first order (PFO) was proposed by Lagergren as a method for investigating the kinetics of adsorption process [46], [60], [61] and can be mathematically expressed in linear and nonlinear forms (equation 4.9 - 4.11):

$$\frac{dq_t}{dt} = k_1(q_e - q_t) \dots \dots \dots (4.9)$$

where,

q_e = the adsorption capacity of the adsorbent at equilibrium (mg/g)

k_1 = pseudo-first order kinetic model rate constant (min⁻¹),

q_t is the amount of adsorbate (gas) adsorbed on the adsorbent at time t .

If we integrate the above equation 4.9 for the boundary conditions of $q_t = 0$ at $t = 0$ and $q_t = q_t$ at $t = t$, we get the following equation.

$$q_t = q_e - q_e e^{-k_1 t} \dots\dots\dots(4.10)$$

By taking a natural logarithm, this equation may also be rewritten as the following linear mathematical expression[46].

$$\ln(q_e - q_t) = \ln q_e - k_1 t \dots\dots\dots(4.11)$$

The values of the pseudo-first order parameters (k_1 and q_e) presented in Table 4.4 were computed using the slope and intercept of the graph plotted as $\ln(q_e - q_t)$ versus t as shown in Fig 4.10a. Comparison of the estimated values of adsorption capacity (q_e) and coefficients of determination (R^2) of the Lagergren pseudo-first and pseudo-second order kinetics revealed that the H_2S adsorption data were best described by the pseudo-first order kinetics model with R^2 value closer to unity (0.9902) and higher and q_e value. On the other hand, the pseudo-first order data in Table 4.4 indicates that the NH_3 and TMA coefficients of determination (R^2) are relatively smaller. In addition, the experimental q_e has relatively bigger difference with the calculated ones,

suggesting that the applicability of the PFO model to the adsorption processes of NH₃ and TMA onto corncob activated carbon is unfeasible.

4.4.2. Pseudo-second Order Kinetics Model

The pseudo-second order (PSO) kinetics model[56], [57], [61]–[65] can be mathematically expressed as the following linear and non-linear equations.

$$\frac{dq_t}{dt} = k_2(q_e - q_t)^2 \dots\dots\dots(4.12)$$

$$q_t = \frac{tk_2q_e^2}{1+tk_2q_e^2} \dots\dots\dots(4.13)$$

$$\frac{t}{q_t} = \frac{1}{k_2q_e^2} + \frac{1}{q_e}t \dots\dots\dots(4.14)$$

The plot of t/q_t against t is shown in Figure 4.10b. The data obtained for the PSO kinetic model is provided in Table 4.4. The pseudo-second order kinetic model revealed good linearity with higher coefficient of determination and lower values of residual sum of square (RSS) for both NH₃ ($R^2 = 0.9943$) and TMA ($R^2 > 0.9771$). Furthermore, in the pseudo-second order model, low deviation was observed between the calculated q_e values and the experimental $q_{e, \text{exp}}$ values for NH₃ and TMA.

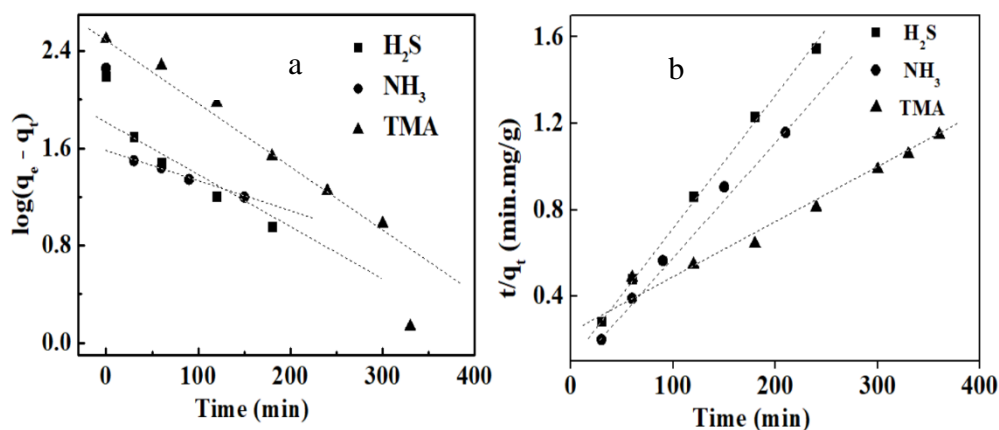


Figure 4.10. Kinetics study. (a) Pseudo-first order kinetics of H₂S, NH₃ and TMA, (b) Pseudo-second order kinetics of H₂S, NH₃ and TMA

The values of k_2 and q_e were determined using the slope and intercept of the graph t/q_t versus t . Hence, the analysis of the data in Table 4.4 suggests that the kinetics of the adsorption of NH₃ and TMA onto corncob activated carbon can be explained accurately by the PSO kinetic model.

4.4.3. Intra-particle Diffusion Model

The Weber-Morris intra-particle diffusion model parameters are extensively used to decide if intraparticle diffusion is the rate limiting step[37][66].

$$q_t = k_i t^{1/2} + C_i \dots \dots \dots (4.15)$$

The model proposes that if the adsorption process is mainly controlled by the intraparticle diffusion, the plot of q_t against $t^{1/2}$ gives linear plot and passes through the origin. When more than two factors control the adsorption process, the plot of q_t versus $t^{1/2}$ will be multi-linear[17]. Fig 4.11 shows the graph of intraparticle model, i.e. q_t vs. $t^{1/2}$. Given the multi-linear nature of the plot for the three gaseous adsorbents, it is proposed that adsorption occurred in two distinct phases: a fast initial uptake during the first stage, followed by slower increase for the second stage until equilibrium is reached. Initially, the abundance of vacant and easy accessible adsorption sites led to high rate of H_2S , NH_3 and TMA adsorption.

Adsorption rate in this stage is mainly controlled by the external diffusion at the boundary layer. Then, adsorption rate of the three-adsorbate gases slowly dropped due to the occupation of the easily accessible adsorption sites available on the external activated carbon surface. In addition, the decrease of adsorbate gas concentration led to a slower rate of gas adsorption.

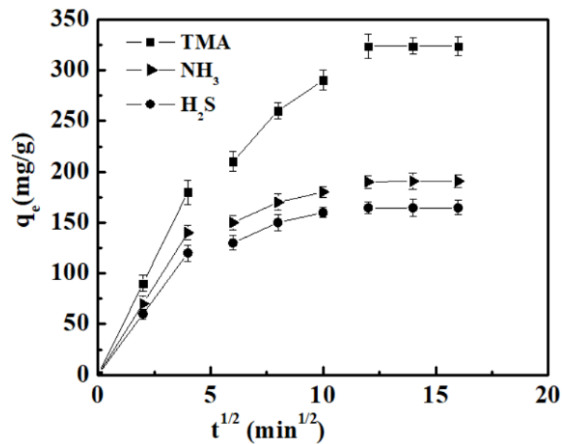


Figure 4.11. Intraparticle diffusion model for the adsorption of H₂S, NH₃ and TMA

The horizontal plateau is an indication of the attainment of the maximum adsorption capacity. The time needed to reach equilibrium, is the point at which adsorption began to stabilize the adsorption process. When equilibrium was attained, majority of the vacant site get occupied and adsorption becomes difficult due to the repulsive forces between gas adsorbed on AC surface and gas in the outside adsorption box.

Table 4.4 Kinetic parameters, constants and coefficients of determination of H₂S, NH₃ and TMA

| Kinetic Model | Parameters | Values | | |
|-------------------------------|---------------------|------------------|-----------------|------------|
| | | H ₂ S | NH ₃ | TMA |
| Experimental | q _{e,exp} | 154.96 | 181.24 | 313.27 |
| Pseudo-first order | q _{e,calc} | 149.52 | 86.73 | 445.77 |
| | k ₁ | 0.0144 | 0.0136 | 0.0147 |
| | RSS | 0.000157 | 0.07908 | 0.078 |
| | R ² | 0.9902 | 0.6824 | 0.9310 |
| Pseudo-second order | q _{e,calc} | 98.47 | 186.92 | 334.78 |
| | k ₂ | 9.83e-4 | 4.3053e-4 | 1.82384e-5 |
| | RSS | 0.00232 | 0.000233 | 0.0011 |
| | R ² | 0.9219 | 0.9943 | 0.9771 |
| Intraparticle Diffusion Model | k _i | 3.484 | 4.2352 | 6.1412 |
| | C _i | 100.33 | 117.56 | 198.29 |
| | R ² | 0.9651 | 0.9919 | 0.9401 |
| | RSS | 1.5 | 0.256 | 8.16 |

4.5. Filter Regeneration Process

In order to make an adsorption technique to competent with other currently available techniques, it should be environment friendly and economically advantageous. Thus, the recycling and successive regeneration and reuse of adsorbent are crucial issues from economic and environmental point of view. Hence, this work was dedicated to examine the feasibility of

thermal regeneration of the spent activated carbon. Results of H₂S, NH₃ and TMA desorption using mild heat treatment is shown in Figure. 4.12. In this study, a desorption experiments were conducted using heat treatment of the spent CAC450-800 filter in a tubular horizontal electric furnace at 220 °C based on previous study [5].

The desorption was performed using an argon as a purge gas. The argon gas could dislodge the adsorbed gases from the spent activated carbon pores. Because the weak Van der Waals forces are mainly used to attach the gases on the pores of the activated carbon[67], the argon gas could easily displace the adsorbed gases as the molecular vibration persists during heat treatment. Then the adsorbed gases were released and easily swept by the flowing argon gas. The argon gas also prevented the spent activated carbon from burning. The adsorption experiment conducted with the regenerated activated carbon reveals that the regenerated filter has good adsorption potential towards NH₃ and H₂S.

Five consecutive regeneration cycles were carried out and 400-ppm initial concentration of each gas adsorbate was used in every cycle. The adsorption results are graphically presented as removal efficiency versus regeneration cycles as shown in Fig. 12. As Fig. 12 depicts, it is quite evident that the trend of adsorption efficiencies of the three gases are superb, even after repetitive several regeneration cycles. After five cycles, the adsorption efficiency of CAC450-800 was approximately 70, 65, and 60% for ammonia,

hydrogen sulfide and trimethylamine respectively. The decrease of removal efficiency from 100% to 70%, 65%, 60% for ammonia, hydrogen sulfide and trimethylamine respectively after five successive cycles could be attributed to the blockage of pores due to chemisorption, which hinders incomplete desorption[50]. Other causes of this loss of adsorption capacity could arise from the internal reorganization of the activated carbon and collapse of pores during the thermal treatment.

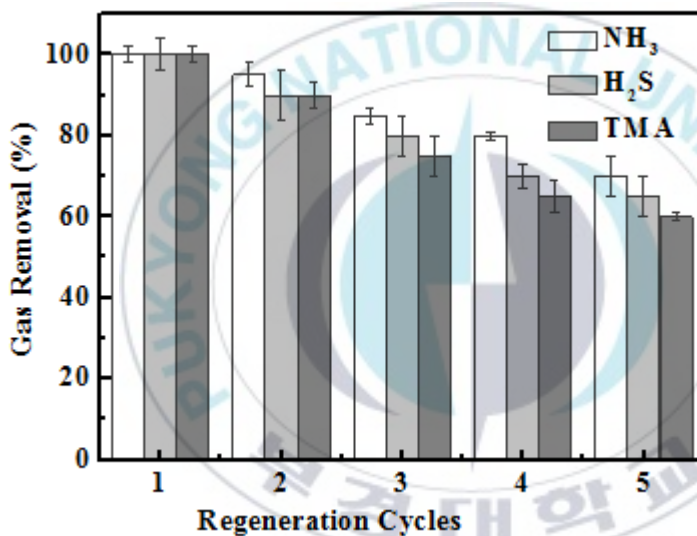


Figure 4.12. Adsorption performance of a regenerated corncob activated carbon filter

5. Conclusions

The copper impregnated corncob activated carbon filter was assessed for its H₂S, NH₃ and TMA adsorption potential for an indoor application. The role of the copper metal was apparent from the superb removal potential of H₂S, NH₃ and TMA compared to the metal unloaded corncob activated carbon. The adsorption isotherm model of the H₂S, NH₃ and TMA was best defined by the Langmuir isotherm model, which indicates that the monolayer surface adsorption was very dominant with acceptable parameters. Adsorption kinetic studies revealed that pseudo-second order kinetic model best described the NH₃ and TMA adsorption whereas pseudo-first order model best described the H₂S adsorption model. Due to its large surface area, cost-effective, numerous micro porosity, and excellent adsorption capacity, the corncob activated carbon is a promising adsorbent for indoor air purification.

The following points have been forwarded for future research. The adsorption test conditions of research are quite different from the conditions typically encountered in indoor spaces. Higher H₂S, NH₃ and TMA concentrations were used during the experiment compared to the real indoors. An airtight small chamber was used for short period of time in the test while the actual indoor area is bigger that needs long term operating filters with enough air exchange. To this end, to determine the performance of an

improved activated carbon filter in actual indoor environment, additional experiments, including long-term tests of the filter life-time as well as the removal efficiencies in actual indoor concentrations of H₂S, NH₃ and TMA will be necessary. Moreover, a single component adsorption experiment was conducted in this work. However, actual indoor areas may compose various pollutants with different concentrations. Hence, a multi-component system of adsorption should be conducted. The effect of levels of humidity and temperature also should be considered.



References

- [1] P. Amoatey, H. Omidvarborna, M. S. Baawain, and A. Al-mamun, "Indoor air pollution and exposure assessment of the gulf cooperation council countries : A critical review," *Environ. Int.*, Vol. 121, No. August, pp. 491–506, 2018.
- [2] J. Young *et al.*, "Development of an activated carbon filter to remove NO₂ and HONO in indoor air," *J. Hazard. Mater.*, Vol. 289, No. 2, pp. 184–189, 2015.
- [3] D. P. Bernabe, R. A. S. Herrera, B. T. D. Jr., M.-L. Fu, Y. Dong, and Y.-F. Wang, "Adsorption of low concentration formaldehyde in air using ethylene-diamine- modified diatomaceous earth," *Aerosol Air Qual. Res.*, Vol. 15, No. 4, pp. 1652–1661, 2015.
- [4] R. Ligotski, U. Sager, U. Schneiderwind, C. Asbach, and F. Schmidt, "Prediction of VOC adsorption performance for estimation of service life of activated carbon based filter media for indoor air purification," *Build. Environ.*, Vol. 149, No. December 2018, pp. 146–156, 2019.
- [5] H. Nama, S. Wang, and H.-R. Jeong, "TMA and H₂S gas removals using metal loaded on rice husk activated carbon for indoor air purification," *Fuel*, Vol. 213, No. July 2017, pp. 186–194, 2018.

- [6] A. Y. A. Takahiro Hirano, Hiroshi Kurosawa, Kazuo Nakamura, “Simultaneous removal of hydrogen sulfide and trimethylamine by a bacterial deodorant,” *J. Ferment. Bioeng.*, Vol. 81, No. 4, pp. 337–342, 1996.
- [7] H. N. T. Mai Thi Vu, Huan-Ping Chao, Tuyen Van Trinh, Trinh Thi Le, Chu-Ching Lin, “Removal of ammonium from groundwater using NaOH-treated activated carbon derived from corncob wastes: Batch and column experiments,” *J. Clean. Prod.*, Vol. 180, pp. 560–570, 2018.
- [8] J. E. Weihua Zheng, Jingtian Hu, Sammuel Rappeport, Zhen Zheng, Zixing Wang, Zheshen Han, James Langer, “Activated carbon fiber composites for gas phase ammonia adsorption,” *Microporous Mesoporous Mater.*, Vol. 234, pp. 146–154, 2016.
- [9] C. L. Qing Fu, Binghui Zheng, Xingru Zhao, Lijing Wang, “Ammonia pollution characteristics of centralized drinking water sources in China,” *J. Environ. Sci.*, Vol. 24, No. 10, pp. 1739–1743, Oct. 2012.
- [10] M. N. Ebrahim Rezaei, Ruth Azar and Bernardo Predicala, “Gas phase adsorption of ammonia using nano TiO₂-activated carbon composites – Effect of TiO₂ loading and composite characterization,” *J. Environ. Chem. Eng.*, Vol. 5, No. 6, pp. 5902–5911, 2017.

- [11] T. Mochizuki, M. Kubota, H. Matsuda, and L. D'EliaCamacho, "Adsorption behaviors of ammonia and hydrogen sulfide on activated carbon prepared from petroleum coke by KOH chemical activation," *Fuel Process. Technol.*, Vol. 144, pp. 164–169, 2016.
- [12] L. Pokorna-Krayzelova *et al.*, "Separation and Purification Technology The use of a silicone-based biomembrane for microaerobic H₂S removal from biogas," *Sep. Purif. Technol.*, Vol. 189, No. March, pp. 145–152, 2017.
- [13] L. Ruiz-Rodríguez, T. Blasco, E. Rodríguez-Castellón, and José M. López Nieto, "Partial oxidation of H₂S to sulfur on V-Cu-O mixed oxides bronzes," *Catal. Today*, No. July, 2018.
- [14] M. J. Jafari *et al.*, "Experimental optimization of a spray tower for ammonia removal," *Atmos. Pollut. Res.*, Vol. 9, No. 4, pp. 783–790, 2018.
- [15] X. L. Qinan Song, Miao Li, Lele Wang, Xuejiao Ma, Fang Liu, "Mechanism and optimization of electrochemical system for simultaneous removal of nitrate and ammonia," *J. Hazard. Mater.*, Vol. 363, No. September 2018, pp. 119–126, 2019.
- [16] G. Shang, G. Shen, L. Liu, Q. Chen, and Z. Xu, "Kinetics and mechanisms of hydrogen sulfide adsorption by biochars," *Bioresour. Technol.*, Vol. 133, pp. 495–499, 2013.

- [17]Y. Y. Fen Li, Tao Le, Yanping Zhang, Jinzhi Wei, "Preparation, characterization of sludge adsorbent and investigations on its removal of hydrogen sulfide under room temperature," *Front. Environ. Sci. Eng.*, Vol. 9, No. 2, Apr. 2013.
- [18]Léa Sigot, Gaëlle Ducom, and Patrick Germain, "Adsorption of hydrogen sulfide (H₂S) on zeolite (Z): Retention mechanism," *Chem. Eng. J.*, Vol. 287, pp. 47–53, 2016.
- [19]K. Ge, Y. Wu, T. Wang, and J. Wu, "Separation and Purification Technology Humidity swing adsorption of H₂S by fibrous polymeric ionic liquids (PILs)," *Sep. Purif. Technol.*, Vol. 217, No. 38, pp. 1–7, 2019.
- [20]S. Xiao-mei, Z. Shu-quan, and Z. Wen-hui, "Effect of surface modification of activated carbon on its adsorption capacity for NH₃," *J. China Univ. Min. Technol.*, Vol. 18, No. October 2007, pp. 0261–0265, 2008.
- [21]A. Tsedeke *et al.*, "Factors that transformed maize productivity in Ethiopia," *Springer*, Vol. 7, pp. 965–981, 2015.
- [22]J. Zhua, Y. Lia, L. Xua, and Z. Liua, "Ecotoxicology and Environmental Safety Removal of toluene from waste gas by adsorption-desorption process using corncob-based activated carbons as adsorbents," *Ecotoxicol. Environ. Saf.*, Vol. 165, No. 135, pp. 115–125, 2018.

- [23]G. O. El-Sayed, M. M. Yehia, and A. A. Asaad, "Assessment of activated carbon prepared from corncob by chemical activation with phosphoric acid," *Water Resour. Ind.*, Vol. 7–8, pp. 66–75, 2014.
- [24]D. Wang, Z. Geng, C. Zhanga, X. Zhoua, and X. Liu, "Effects of thermal activation conditions on the microstructure regulation of corncob-derived activated carbon for hydrogen storage," *J. Energy Chem.*, Vol. 23, No. 5, pp. 601–608, Sep. 2014.
- [25]V. O. Njoku and B.H. Hameeda, "Preparation and characterization of activated carbon from corncob by chemical activation with H₃PO₄for 2,4-dichlorophenoxyacetic acid adsorption," *Chem. Eng. J.*, Vol. 173, No. 2, pp. 391– 399, 2011.
- [26]A. Amphol, Paitip Thiravetyanb, and W. Nakbanpote, "Preparation of CO₂ activated carbon from corncob for monoethylene glycol adsorption," *Colloids Surfaces A Physicochem. Eng. Asp.*, Vol. 333, No. 1–3, pp. 19–25, Feb. 2009.
- [27]M. F. P. Latiff, Abustan, M.A.Ahmad, N. K. E. . Yahaya, and A.M.khalid, "Effect of preparation conditions of activated carbon prepared from corncob by CO₂ activation for removal of Cu (II) from aqueous solution," *Am. Inst. Phys.*, vol. 030001, No. Ii, pp. 145–152, 2016.

- [28]David M. Newman, *May 2016 Dirty and Dangerous Worker Safety and Health in New York City 's*, no. May. New York City: New York Committee for Occupational Safety and Health, 2016.
- [29]National Research Council of the National Academies, *Acute Exposure Guideline Levels for Selected Airborne Chemicals: vol. 6*. Washington, D.C: National Academies Press, 2007.
- [30]R. F. Griffiths, "Production of dense gas mixtures from ammonia releases - A review," *J. Hazard. Mater.*, Vol. 6, No. 1–2, pp. 197–212, 1982.
- [31]The Fertilizer Institute, "Health Effects of Ammonia," 2018, p. 22.
- [32]Phattara Boraphech and P. Thiravetyan, "Trimethylamine (fishy odor) adsorption by biomaterials: Effect of fatty acids, alkanes, and aromatic compounds in waxes," *J. Environ. Sci.*, Vol. 79, No. 284, pp. 269–277, 2018.
- [33]G. Shang, G. Shen, L. Liu, and Z. X. Qin Chen, "Bioresource Technology Kinetics and mechanisms of hydrogen sulfide adsorption by biochars," *Bioresour. Technol.*, Vol. 133, pp. 495–499, 2013.
- [34]E. Rezaei, B. Schlageter, M. Nemati, and B. Predicala, "Evaluation of metal oxide nanoparticles for adsorption of gas phase ammonia," *J. Environ. Chem. Eng.*, Vol. 5, No. 1, pp. 422–431, 2017.

- [35]W. Zheng *et al.*, “Microporous and Mesoporous Materials Activated carbon fiber composites for gas phase ammonia adsorption,” *Microporous Mesoporous Mater.*, Vol. 234, pp. 146–154, 2016.
- [36]M. A. El Zayat, “Removal of Heavy Metals by Using Activated Carbon Produced from Cotton Stalks,” The American University in Cairo, 2009.
- [37]B. I., P. N. D. Olu-Owolabi a, and K. O. Adebowale, “Evaluation of pyrene sorption-desorption on tropical soils,” *J. Environ. Manage.*, Vol. 137, pp. 1–9, 2014.
- [38]A. L. Yaumi, M. Z. A. Bakar, and B. H. Hameed, “Melamine-nitrogenated mesoporous activated carbon derived from rice husk for carbon dioxide adsorption in fixed-bed,” *Energy*, Vol. 155, pp. 46–55, Jul. 2018.
- [39]S. Amir, “Production of activated carbon within the indirect gasification process,” Chalmers University of Technology, 2012.
- [40]M. Song *et al.*, “The comparison of two activation techniques to prepare activated carbon from corn cob,” *Biomass and Bioenergy*, Vol. 48, pp. 250–256, 2013.
- [41]M. K. B. Gratuito, T. Panyathanmaporn, R. A. Chumnanklang, N. Sirinuntawittaya, and A. Dutta, “Production of activated carbon from coconut shell: Optimization using response surface methodology,” *Bioresour. Technol.*, Vol. 99, No. 11, pp. 4887–4895, 2008.

- [42]D. Li, C. Li, Y. Tian, L. Kong, and L. Liu, “Influences of impregnation ratio and activation time on ultramicropores of peanut shell active carbons,” *Mater. Lett.*, Vol. 141, pp. 340–343, 2015.
- [43]N. Bagheri and J. Abedi, “Preparation of high surface area activated carbon from corn by chemical activation using potassium hydroxide,” *Chem. Eng. Res. Des.*, Vol. 87, No. 8, pp. 1059–1064, 2009.
- [44]I. G. Council, “Market Report.” International Grain Council, London, p. 10, 2019.
- [45]X. Liu, C. Zhang, Z. Geng, and M. Cai, “High-pressure hydrogen storage and optimizing fabrication of corncob-derived activated carbon,” *Microporous Mesoporous Mater.*, Vol. 194, pp. 60–65, 2014.
- [46]J. Mohammed, N. S. Nasri, M. A. A. Zaini, U. D. Hamza, and F. N. Ani, “Adsorption of benzene and toluene onto KOH activated coconut shell based carbon treated with NH_3 ,” *Int. Biodeterior. Biodegrad.*, Vol. 102, pp. 245–255, 2015.
- [47]S. M. Anisuzzaman, C. G. Joseph, W. M. A. B. W. Daud, D. Krishnaiah, and H. S. Yee, “Preparation and characterization of activated carbon from *Typha orientalis* leaves,” *Int. J. Ind. Chem.*, Vol. 6, No. 1, pp. 9–21, 2015.
- [48]R. R. Gil, B. Ruiz, M. S. Lozano, M. J. Martín, and E. F. A, “VOCs removal by adsorption onto activated carbons from biocollagenic

- wastes of vegetable tanning,” *Chem. Eng. J.*, Vol. 245, pp. 80–88, 2014.
- [49]H. Hadjar, B. Hamdi, and C. O. Aniac, “Adsorption of p-cresol on novel diatomite/carbon composites,” *J. Hazard. Mater.*, Vol. 188, no. 1–3, pp. 304–310, Apr. 2011.
- [50]D. Bhattacharjya and J.-S. Yu, “Activated carbon made from cow dung as electrode material for electrochemical double layer capacitor,” *J. Power Sources*, Vol. 262, pp. 224–231, 2014.
- [51]E. Altintig, Gulnur Arabaci, and Huseyin Altundag, “Preparation and characterization of the antibacterial efficiency of silver loaded activated carbon from corncobs,” *Surf. Coat. Technol.*, Vol. 304, pp. 63–67, 2016.
- [52]H. Hwang, O. Sahin, and J. W. Choi, “RSC Advances Manufacturing a super-active carbon using fast pyrolysis char from biomass and correlation study on structural features and phenol adsorption” *R. Soc. Chem.*, vol. 7, no. 42192, pp. 42192–42202, 2017.
- [53]A. . Dada, A. . Olalekan, A. . Olatunya, and O. DADA, “Langmuir, Freundlich, Temkin and Dubinin–Radushkevich Isotherms Studies of Equilibrium Sorption of Zn^{2+} onto Phosphoric Acid Modified Rice Husk,” *IOSR J. Appl. Chem.*, Vol. 3, No. 1, pp. 38–45, 2012.

- [54]B. H. Hameed, A. T. M. Din, and A. L. Ahmad, “Adsorption of methylene blue onto bamboo-based activated carbon: Kinetics and equilibrium studies,” *J. Hazard. Mater.*, Vol. 141, pp. 819–825, 2007.
- [55]F. Gironia and V. Piemonte, “VOCs removal from dilute vapour streams by adsorption onto activated carbon,” *Chem. Eng. J.*, Vol. 172, No. 2–3, pp. 671– 677, 2011.
- [56]S. Bousb and A. H. Meniai, “Adsorption of 2-chlorophenol onto sewage sludge based adsorbent: Equilibrium and kinetic study,” *Chem. Eng. Trans.*, Vol. 35, pp. 1974–9791, 2013.
- [57]F. Ferrero, “Adsorption of Methylene Blue on magnesium silicate: Kinetics, equilibria and comparison with other adsorbents,” *J. Environ. Sci.*, Vol. 22, No. 3, pp. 467–473, 2010.
- [58]C.-J. Sun, L.-Z. Sun, and X.-X. Sun, “Graphical Evaluation of the Favorability of Adsorption Processes by Using Conditional Langmuir Constant,” *J. Ind. Eng. Chem. Res.*, Vol. 52, p. 14251–14260, 2013.
- [59]Mohamed Erhayem, Fatima Al-Tohami, R. Mohamed, and KhadijaAhmida, “Isotherm, Kinetic and Thermodynamic Studies for the Sorption of Mercury (II) onto Activated Carbon from Rosmarinus officinalis Leaves,” *Am. J. Anal. Chem.*, Vol. 6, No. 6, pp. 1–10, 2015.

- [60]C. Sauciera *et al.*, “Microwave-assisted activated carbon from cocoa shell as adsorbent for removal of sodium diclofenac and nimesulide from aqueous effluents,” *J. Hazard. Mater.*, Vol. 289, 2015.
- [61]M. Aivalioti, Ioannis Vamvasakis, and E. Gidarakos, “BTEX and MTBE adsorption onto raw and thermally modified diatomite,” *J. Hazard. Mater.*, Vol. 178, No. 1–3, pp. 136–143, 2010.
- [62]E. Da’na and A. Awad, “Regeneration of spent activated carbon obtained from home filtration system and applying it for heavy metals adsorption,” *J. Environ. Chem. Eng.*, Vol. 5, No. 4, pp. 3091–3099, 2017.
- [63]W.-T. Tsai, Chi-Wei Lai, and K.-J. Hsien, “Characterization and adsorption properties of diatomaceous earth modified by hydrofluoric acid etching,” *J. Colloid Interface Sci.*, Vol. 297, No. 2, pp. 749–754, 2006.
- [64]J. X. L. S. L. Z. A. M. H. F. A. X. Q. Qian, “The adsorption of dyes from aqueous solution using diatomite,” *J. Porous Mater.*, Vol. 14, No. 4, pp. 449–455, 2007.
- [65]B. Salim Bousbaa and A. H. Meniai, “Removal of phenol from water by adsorption onto sewage sludge based adsorbent,” *Chem. Eng. Trans.*, Vol. 40, no. Special Issue, pp. 235–240, 2014.
- [66]T. Tarawou and E. Young, “Intraparticle and Liquid film Diffusion Studies on the Adsorption of Cu^{2+} and Pb^{2+} Ions from Aqueous

Solution using Powdered Cocoa Pod (*Theobroma cacao*),” *Int. Res. J. Eng. Technol.*, Vol. 02, No. 2395, 2015.

[67]H. S. Choo, L. C. Lau, A. R. Mohamed, and K. T. Lee, “Hydrogen Sulfide Adsorption by Alkaline Impregnated Coconut Shell Activated Carbon,” *J. Eng. Sci. Technol.*, Vol. 8, No. 6, pp. 741–753, 2013.



Acknowledgement

First, I would like to thank the Almighty GOD with a humble heart, for providing me the strength and blessings to pursue my master study abroad with His grace.

Next, I am greatly indebted to my academic Advisor, Prof. Ki Woo Nam. If it wasn't for his patience and believing in me, I wouldn't be graduating now. His constant support, personal care and insightful suggestions were instrumental in completing my study.

No word of thanks will be enough to convey my gratitude to my senior labmate Shuang Wang for his invaluable advice and guidance with constant encouragement and continuous support throughout my master study. I owe him lots of gratitude for his continued supervision, advice and guidance throughout the study. I will always remember his true friendliness and kindness.

The words are also boundless to express my gratitude to Yea Na Lee, Sung Min Jung, Byeong Su Kim, Hye Jin Yang, Mi Hyang Park, Min Heon Kim, Jaen Paeng, Jangwon Lee and Taeyeong Kim, all the crew member of Strength of Materials Laboratory for their true friendship, moral support, care, affection and encouragement, which gave me the spirit and courage both for my academic and social life.

I'd also like to thank my thesis review committee members Dr. Jun Heok Lim and Dr. Hee Rok Jeong for their supportive guidance in finishing this dissertation. Their insightful suggestions and constructive criticisms also broadened my professional experience.

I am also grateful to professors of Pukyong National University central laboratory, who provided me help with material characterization particularly SEM, EDS, TGA, and Nitrogen adsorption experiments.

My acknowledgement would be incomplete without mentioning the biggest source of my strength, all my families and friends, who were on my side throughout my study.

Last but not least, my sincere appreciation goes to the government of the Republic of Korea for providing me scholarship to pursue my graduate study. I am deeply honored to be one of the recipients of the Global Korean Scholarship Program, which provided me the financial supports throughout my study.